Published for SISSA by Springer

Received: November 16, 2021
Accepted: March 1, 2022
Published: March 21, 2022

Higher-order non-global logarithms from jet calculus

Andrea Banfi,[a] **Frédéric A. Dreyer**[b] **and Pier Francesco Monni**[c]

[a] *Department of Physics and Astronomy, University of Sussex, Sussex House, Brighton, BN1 9RH, U.K.*

[b] *Rudolf Peierls Centre for Theoretical Physics, Clarendon Laboratory, Parks Road, Oxford OX1 3PU, U.K.*

[c] *Theoretical Physics Department, CERN, CH-1211 Geneva 23, Switzerland*

E-mail: a.banfi@sussex.ac.uk, frederic.dreyer@physics.ox.ac.uk, pier.monni@cern.ch

Abstract: Non-global QCD observables are characterised by a sensitivity to the full angular distribution of soft radiation emitted coherently in hard scattering processes. This complexity poses a challenge to their all-order resummation, that was formulated at the leading-logarithmic order about two decades ago. In this article we present a solution to the long-standing problem of their resummation beyond this order, and carry out the first complete next-to-leading logarithmic calculation for non-global observables. This is achieved by solving numerically the recently derived set of non-linear differential equations which describe the evolution of soft radiation in the planar, large-N_c limit. As a case study we address the calculation of the transverse energy distribution in the interjet rapidity region in $e^+e^- \to$ dijet production. The calculation is performed by means of an algorithm that we formulate in the language of jet-calculus generating functionals, which also makes the resummation technique applicable to more general non-global problems, such as those that arise in hadronic collisions. We find that NLL corrections are substantial and their inclusion leads to a significant reduction of the perturbative scale uncertainties for these observables. The computer code used in the calculations is made publicly available.

Keywords: Jets, QCD Phenomenology

ArXiv ePrint: 2111.02413

https://doi.org/10.1007/JHEP03(2022)135

Contents

1 Introduction

The topic of non-global QCD observables [1] has received significant attention in recent years. A first reason is due to their theoretical complexity. These observables are characterised by kinematic constraints on limited angular regions of the radiation phase space, which leads to a rich structure in perturbation theory. This class of logarithmic corrections to physical observables was discovered and resummed at leading logarithmic (LL) order in the planar, large-number-of-colour (large-N_c) limit about 20 years ago [1–3], and methods to calculate finite-N_c effects are also well established [4–8]. While subleading-colour corrections are commonly numerically small in known applications, their study is of importance for the understanding of the structure of super-leading logarithmic corrections in non-global observables at hadron colliders [9–11].

The calculation of non-global corrections to higher orders largely remains an open problem. Several new formulations of the resummation have been proposed in recent years [12–16], accompanying a large amount of applications to perturbative calculations of collider observables at LL, and recently also including some class of NLL corrections (see e.g. [12, 17–34]). Their study is also motivated by theoretical interests related to the connection between their dynamics and the high-energy limit of scattering amplitudes [14, 35, 36].

A second reason why non-global observables are interesting is their ubiquitous occurence at colliders, for instance via the use of jets or often when specific fiducial cuts are

JHEP03(2022)135

applied in experimental measurements. In the context of the precision physics programme of present and future particle colliders, it is therefore paramount to gain theoretical control over non-global corrections to physical observables.

Finally, an understanding of their dynamics is instrumental in the context of developing more accurate parton-shower algorithms (see e.g. refs. [37–48]). Specifically, the resummation of next-to-leading logarithmic (NLL) non-global logarithms is a crucial ingredient for the development of NNLL algorithms, that are necessary to achieve sufficiently accurate event simulation both at present and future colliders.

In a recent article [16] we have developed a framework for the resummation of non-global observables in the planar limit, which relies on a set of non-linear evolution equations that describe the dynamics of soft radiation at different energy scales. Ref. [16] also demonstrates the correctness of the framework by comparing a calculation at fixed perturbative order in this formalism to the full QCD result for the energy and transverse energy distributions in the rapidity gap between two cone jets produced in electron-positron annihilation.

In this article, we instead address the solution of the equations of ref. [16] at all perturbative orders, hereby achieving a first complete NLL resummation for a non-global observable in the large-N_c limit. The paper is structured as follows. Section 2 contains a summary of the findings of ref. [16]. Section 3 reformulates the evolution equations in terms of a well known method used in jet calculus, that of generating functionals [49–51]. This formulation has two important advantages. Firstly, it provides us with a probabilistic picture to solve the evolution equations using a Markov chain Monte-Carlo algorithm. Secondly, the resulting algorithm describing the evolution of the soft radiation in the planar limit is *independent* of the underlying hard scattering process, and therefore can be readily applied to other observables and reactions, such as jet production at hadron colliders. The algorithm is given in detail in section 4, which is arguably the most technical part of the article. The reader uninterested in the technical aspects of the calculation can skip directly from section 3 to section 5 where the numerical results are presented. In section 5 we report NLL predictions for the transverse energy distribution in the interjet rapidity slice in $e^+e^- \to 2$ jets, and discuss the impact of NLL corrections as well as the reduction in the perturbative uncertainty. Finally, section 6 contains our conclusions.

2 Resummation for E_t in the interjet rapidity gap

As in ref. [16], we consider the production of two jets in e^+e^- annihilation at a centre-of-mass energy $\sqrt{s}$. We study a non-global observable defined by measuring hadrons in a rapidity slice between the two jets. This is defined as the rapidity region between two cones of opening angle θ_{jet} around the thrust axis (see figure 1). The width of such a rapidity slice is

$$\Delta\eta := \ln\frac{1+c}{1-c}, \qquad c = \cos\theta_{\text{jet}}\,. \tag{2.1}$$

Examples of non-global observables are those studied in ref. [16], namely the total energy or transverse energy of hadrons inside the slice. In the following we consider the latter for the sake of arguments, although the formalism introduced in this section also applies to the calculation of the energy distribution.

JHEP03(2022)135

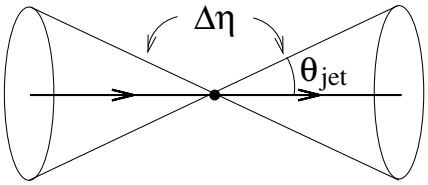

Figure 1. The rapidity slice where the measurement is performed.

The cumulative distribution for this observable to be less than $v \equiv E_t$ is defined as follows

$$\Sigma(v) \coloneqq \frac{1}{\sigma_0} \int_0^v \frac{d\sigma}{dv'} dv' \,, \tag{2.2}$$

where σ_0 is the Born cross section for $e^+e^- \to$ hadrons. In the limit $v \ll \sqrt{s}$, large logarithms $L = \ln(\sqrt{s}/v)$ spoil the convergence of fixed-order perturbative expansions and must be resummed at all perturbative orders. Since this observable is affected only by soft emissions at wide angles, the largest logarithms in $\Sigma(v)$, the leading logarithms, are of the form $\alpha_s^n L^n$. For $\alpha_s L \sim 1$, all terms suppressed by an extra power of α_s give next-to-leading logarithmic (NLL, $\alpha_s^n L^{n-1}$) contributions, and so on. Without any emissions, at the lowest order in perturbation theory, $\Sigma(v) = 1$, and the event is made up of a quark of momentum p_1 and an antiquark of momentum p_2, back-to-back and aligned along the thrust axis. When extra radiation is considered, $\Sigma(v)$ can be expressed as [16]

$$\Sigma(v) \coloneqq \sum_{n=2}^{\infty} \mathcal{H}_n \otimes S_n(v) = \mathcal{H}_2 \otimes S_2(v) + \mathcal{H}_3 \otimes S_3(v) + \cdots \tag{2.3}$$

where the hard factors

$$\mathcal{H}_n \coloneqq \mathcal{H}_{1\ldots n} \tag{2.4}$$

describe configurations with n hard QCD partons along the light-like directions $n_1, \ldots, n_n$ (with $n_i^2 = 0$ and $|\vec{n}|^2 = 1$), while the soft factors

$$S_n \coloneqq S_{1\ldots n} \tag{2.5}$$

describe the emission of soft radiation off a hard system with n hard emitters along the same directions. The convolutions in eq. (2.3) are meant to indicate that the directions of the hard emitters in the hard and soft factors are the same, namely

$$\mathcal{H}_n \otimes S_n(v) \coloneqq \int \left(\prod_{i=i}^{n} d^2\Omega_i \right) \mathcal{H}_{1\ldots n} \times S_{1\ldots n}(v), \tag{2.6}$$

where Ω_i indicates the solid angle of the i-th hard emitter, namely the direction of the $\vec{n}_i$ vector, specified by a longitudinal (θ) and an azimuthal (ϕ) angle. In writing eq. (2.6) we assumed that all IRC divergences cancel in the definition of $\mathcal{H}_n$ and S_n, and the four-dimensional limit can be taken in the angular integration [16]. Each of the above ingredients admits a perturbative expansion in the strong coupling constant [16]

$$\mathcal{H}_n = \sum_{i=n-2}^{\infty} \frac{\alpha_s^i}{(2\pi)^i} \mathcal{H}_n^{(i)}, \qquad S_n = \sum_{i=0}^{\infty} \frac{\alpha_s^i}{(2\pi)^i} S_n^{(i)}, \tag{2.7}$$

JHEP03(2022)135

where the normalisation is defined such that at the Born level one has

$$\mathcal{H}_2^{(0)} = \delta^{(2)}(\Omega_1 - \Omega_q)\delta^{(2)}(\Omega_2 - \Omega_{\bar{q}}) \coloneqq \delta(\cos\theta_1 - 1)\delta(\cos\theta_2 + 1)\delta(\phi_1)\delta(\phi_2)\,, \quad S_n^{(0)} = 1\,. \tag{2.8}$$

At LL, the cumulative distribution is given by the convolution of the LO hard factor $\mathcal{H}_2$ with the LL soft factor S_2. At NLL, one needs to include the LO hard factor $\mathcal{H}_3$ convoluted with the LL soft factor S_3, as well as the NLO hard factor $\mathcal{H}_2$ convoluted with the NLL soft factor S_2.

The observables considered in ref. [16] were all additive, which implies that the observable constraint on the soft emissions contributing to S_n factorises under the Laplace transform

$$\Theta\left(v - \sum_i V(k_i)\Theta_{\text{in}}(k_i)\right) = \frac{1}{2\pi i}\int_\gamma \frac{d\nu}{\nu} e^{\nu v} \prod_i u(k_i)\,, \tag{2.9}$$

where the trigger function $\Theta_{\text{in}}(k)$ is 1 if the particle k is inside the measurement region, and zero otherwise, and the contour γ lies parallel to the imaginary axis and to the right of all singularities of the integrand. The quantity $u(k)$ is the following "source" function:

$$u(k) = \Theta_{\text{out}}(k) + \Theta_{\text{in}}(k)e^{-\nu V(k)}\,, \tag{2.10}$$

with $\Theta_{\text{out}}(k) = 1 - \Theta_{\text{in}}(k)$. Following ref. [16], in the large-N_c limit we can then define the Laplace transform of the soft factors entering the NLL calculation

$$S_2(v) = \frac{1}{2\pi i}\int_\gamma \frac{d\nu}{\nu} e^{\nu v} G_{12}[Q;u]\,, \quad S_3(v) = \frac{1}{2\pi i}\int_\gamma \frac{d\nu}{\nu} e^{\nu v} G_{13}[Q;u]G_{23}[Q;u]\,. \tag{2.11}$$

The evolution of the $G_{ij}[Q;u]$ functionals is governed by the differential equation (in the following we set $\{ij\} = \{12\}$ unless otherwise specified, but the same considerations hold for the evolution of a generic dipole $\{ij\}$)

$$Q\partial_Q G_{12}[Q;u] = \mathbb{K}[G[Q;u],u]\,. \tag{2.12}$$

The evolution kernels are derived in ref. [16], and we report them in $4-2\epsilon$ dimensions below. The LL kernel, relevant for the evolution of S_3 reads

$$\begin{aligned}\mathbb{K}^{\text{LL}}[G[Q;u],u] \coloneqq \int [dk_a]\bar{\alpha}(Q)w_{12}^{(0)}(k_a) \\ \times \left(G_{1a}[Q;u]G_{a2}[Q;u]u(k_a) - G_{12}[Q;u]\right) Q\delta(Q - k_{ta})\,.\end{aligned} \tag{2.13}$$

The tree-level eikonal squared amplitude is defined as

$$w_{ij}^{(0)}(k) = 8\pi^2 \frac{\mu^{2\epsilon}}{k_t^2}\,, \quad k_t^2 \coloneqq (k_t^{(ij)})^2 = 2\frac{(k_i\cdot k)(k\cdot k_j)}{(k_i\cdot k_j)}\,, \tag{2.14}$$

where k_t denotes the transverse momentum of emission k w.r.t. the emitting $\{ij\}$ dipole (note that in the equation above $k_{i,j} \equiv p_{i,j}$ if it refers to one of the hard legs). In the same variables, the corresponding phase space measure in $4-2\epsilon$ dimensions reads

$$[dk] \coloneqq \frac{d\eta}{2}\frac{d^{2-2\epsilon}k_t}{(2\pi)^{3-2\epsilon}}\,, \tag{2.15}$$

JHEP03(2022)135

where the rapidity bound in the soft limit is given by

$$|\eta| \lesssim \ln \frac{\sqrt{2\, k_i \cdot k_j}}{k_t}\,. \tag{2.16}$$

A discussion about the choice of ordering variable and its relation to symmetries of the multi-particle squared amplitude is reported in appendix A. In eq. (2.13) we also defined $\bar{\alpha} = N_c \alpha_s(\mu)/\pi$, where α_s is the QCD coupling in the $\overline{\text{MS}}$ scheme, satisfying the renormalisation group equation (RGE)

$$\frac{d\bar{\alpha}(\mu)}{d\ln\mu^2} = -\bar{\beta}(\bar{\alpha}) = -\bar{\alpha}\left(\bar{\beta}_0\bar{\alpha} + \bar{\beta}_1\bar{\alpha}^2 + \dots\right), \tag{2.17}$$

where $\bar{\beta}_i$ are obtained from the large-N_c limit of the coefficients of the QCD beta function as

$$\bar{\beta}_i = \lim_{N_c\to\infty}\left(\frac{\pi}{N_c}\right)^{i+1}\beta_i\,. \tag{2.18}$$

We work in the normalisation in which $\beta_0 = (11C_A - 2n_F)/(12\pi)$ and $\bar{\beta}_0 = 11/12$. The coupling in the LL kernel (2.13) evolves at one loop (i.e. setting $\bar{\beta}_1 = 0$ in eq. (2.17)), while it evolves at two loops in the NLL kernel defined in the following. The NLL kernel which governs the evolution of S_2 reads

$$\mathbb{K}^{\text{NLL}}[G[Q;u],u] \coloneqq \mathbb{K}^{\text{RV+VV}}[G[Q;u],u] + \mathbb{K}^{\text{RR}}[G[Q;u],u] - \mathbb{K}^{\text{DC}}[G[Q;u],u]\,. \tag{2.19}$$

The three contributions to the above equation describe three sources of NLL corrections. The kernel correction due to the subtracted virtual and real-virtual corrections reads

$$\begin{aligned}\mathbb{K}^{\text{RV+VV}}[G[Q;u],u] \coloneqq \int [dk_a]\bar{\alpha}(Q) w_{12}^{(0)}(k_a)\left(1+\bar{\alpha}(Q)\,\bar{K}^{(1)}\right)\\ \times\left(G_{1a}[Q;u]G_{a2}[Q;u]u(k_a) - G_{12}[Q;u]\right) Q\delta(Q-k_{ta})\,,\end{aligned} \tag{2.20}$$

where $\bar{K}^{(1)}$ is obtained from the two-loop cusp anomalous dimension in the large-N_c limit

$$\bar{K}^{(1)} = \lim_{N_c\to\infty}\frac{2}{N_c}K^{(1)} = \frac{67}{36} - \frac{\pi^2}{12}\,. \tag{2.21}$$

Then, the double real corrections are given by

$$\begin{aligned}\mathbb{K}^{\text{RR}}[G[Q;u],u] \coloneqq \int [dk_a]\int [dk_b]\,\bar{\alpha}^2(Q) Q\delta(Q-k_{t(ab)})\Theta(k_{ta}-k'_{tb})\\ \times\Big[\bar{w}_{12}^{(gg)}(k_b,k_a)G_{1b}[Q;u]G_{ba}[Q;u]G_{a2}[Q;u]u(k_a)u(k_b)\\ +\bar{w}_{12}^{(gg)}(k_a,k_b)G_{1a}[Q;u]G_{ab}[Q;u]G_{b2}[Q;u]u(k_a)u(k_b)\\ -\left(\bar{w}_{12}^{(gg)}(k_b,k_a)+\bar{w}_{12}^{(gg)}(k_a,k_b)\right)G_{1(ab)}[Q;u]G_{(ab)2}[Q;u]u(k_{(ab)})\Big]\,,\end{aligned} \tag{2.22}$$

where k'_{tb} denotes the transverse momentum of k_b with respect of the $\{12\}$ dipole, namely

$$(k'_{tb})^2 = 2\frac{(p_1\cdot k_b)(k_b\cdot p_2)}{(p_1\cdot p_2)}\,. \tag{2.23}$$

JHEP03(2022)135

To properly define $\bar{w}_{12}^{(gg)}(k_a,k_b)$ we need first to introduce the colour-ordered double soft squared amplitude at tree level [52, 53][1]

$$\tilde{w}_{12}^{(0)}(k_a,k_b) = 2\,(2\pi)^4\mu^{4\epsilon}\Bigg[\frac{s_{12}^2}{s_{1a}s_{ab2}s_{1ab}s_{b2}} + \frac{1-\epsilon}{s_{ab}^2}\left(\frac{s_{1a}}{s_{1ab}}+\frac{s_{b2}}{s_{ab2}}-1\right)^2 + \frac{s_{12}}{s_{ab}}\left(\frac{1}{s_{1a}s_{b2}}+\frac{1}{s_{1a}s_{ab2}}+\frac{1}{s_{b2}s_{1ab}}-\frac{4}{s_{1ab}s_{ab2}}\right)\Bigg], \tag{2.24}$$

where the Lorentz invariants $s_{i\ldots k}$ indicate the standard Mandelstam variables. Following [16], we define $\bar{w}_{12}^{(gg)}(k_a,k_b)$ as the correlated contribution to $\tilde{w}_{12}^{(0)}(k_a,k_b)$, as follows

$$\bar{w}_{12}^{(gg)}(k_a,k_b) \coloneqq \tilde{w}_{12}^{(0)}(k_a,k_b) - \frac{1}{2}w_{12}^{(0)}(k_a)w_{12}^{(0)}(k_b)\,, \tag{2.25}$$

where $\frac{1}{2}w_{12}^{(0)}(k_a)w_{12}^{(0)}(k_b)$ represents the independent emission contribution.[2] The counterterm in the r.h.s. of eq. (2.22) is built upon the massless momentum $k_{(ab)}$ defined by the following kinematic map

$$\mathbb{P}:\{k_a,k_b\}\to k_{(ab)} = \left(k_{t(ab)}\cosh\eta_{(ab)}, \vec{k}_{t(ab)}, k_{t(ab)}\sinh\eta_{(ab)}\right), \tag{2.26}$$

where $k_{t(ab)} \coloneqq |\vec{k}_{t(ab)}|$ and $\eta_{(ab)}$ denote the transverse momentum and rapidity of k_a+k_b in the $\{12\}$ dipole rest frame. Eq. (2.26) is expressed in the $\{12\}$ dipole rest frame where the $\{12\}$ dipole is aligned with the z axis. A Lorentz transformation (a rotation followed by a boost) must be then applied to $k_{(ab)}$ to express it in the event frame. Last, we *subtract* the iteration of the LL kernel

$$\begin{aligned}\mathbb{K}^{\rm DC}[G[Q;u],u] \coloneqq& \int[dk_a]\int[dk_b]\bar{\alpha}^2(Q)Q\delta(Q-k_{ta})\Theta(k_{ta}-k_{tb}) \\ &\times\Bigg[w_{12}^{(0)}(k_a)\left(w_{1a}^{(0)}(k_b)-\frac{1}{2}w_{12}^{(0)}(k_b)\right)G_{1b}[Q;u]G_{ba}[Q;u]G_{a2}[Q;u]u(k_a)u(k_b) \\ &+w_{12}^{(0)}(k_a)\left(w_{a2}^{(0)}(k_b)-\frac{1}{2}w_{12}^{(0)}(k_b)\right)G_{1a}[Q;u]G_{ab}[Q;u]G_{b2}[Q;u]u(k_a)u(k_b) \\ &-w_{12}^{(0)}(k_a)\left(w_{1a}^{(0)}(k_b)+w_{a2}^{(0)}(k_b)-w_{12}^{(0)}(k_b)\right)G_{1a}[Q;u]G_{a2}[Q;u]u(k_a)\Bigg].\end{aligned} \tag{2.27}$$

In the above expression, with a little abuse of notation, we denoted with k_{tb} the transverse momentum of k_b with respect to the *emitting* dipole, that is each term should be interpreted as follows

$$w_{ij}^{(0)}(k_b)\Theta(k_{ta}-k_{tb}) \coloneqq w_{ij}^{(0)}(k_b)\Theta(k_{ta}-k_{tb}^{(ij)})\,, \tag{2.28}$$

where $k_{tb}^{(ij)}$ is the transverse momentum of k_b with respect to the "emitting" dipole $\{ij\}$ (see also eq. (2.14))

$$(k_{tb}^{(ij)})^2 = 2\frac{(k_i\cdot k_b)(k_b\cdot k_j)}{(k_i\cdot k_j)}\,, \tag{2.29}$$

[1] We thank Keith Hamilton for an independent derivation of these squared amplitudes.

[2] Note, however, that the separation of the independent contribution is immaterial at the level of the single colour flow, and only makes physical sense at the level of the sum $\tilde{w}_{12}^{(0)}(k_a,k_b)+\tilde{w}_{12}^{(0)}(k_b,k_a)$.

JHEP03(2022)135

with $k_{i,j} \equiv p_{i,j}$ if it refers to one of the hard legs. The quantity G_{ij} satisfies the boundary condition

$$G_{ij}[Q;u] = 1 \text{ for } Q = 0\,, \tag{2.30}$$

and the normalisation $G_{ij}[Q;1] = 1$. In taking the four-dimensional limit of the above equations some care is required since the boundary condition has to be deformed by introducing an appropriate non-perturbative prescription. In this article we consider implementing the following procedure [16]

$$\alpha_s(k) = \alpha_s(Q_0) = 0, \qquad k \leq Q_0\,, \tag{2.31}$$

where Q_0 is defined below (see eq. (4.5)) and it is above the Landau singularity. This simply amounts to modifying the boundary condition (2.30) such that $G_{ij}[Q;u] = 1$ for $Q \leq Q_0$. We also stress that in four dimensions the collinear singularity $k_a \parallel k_b$ in the r.h.s. of eq. (2.27) is regulated by the requirement that at NLL the two soft gluons k_a and k_b cannot be inside the slice simultaneously as this configuration would in the end produce only a NNLL correction.

A comment is in order about the applicability criteria of the evolution equations given in this section. As presented, eq. (2.12) can be used for the resummation of NLL corrections to non-global observables which do not exhibit logarithmic sensitivity to configurations in which the soft gluons are radiated collinear to the emitting leg, which translates into the absence of Sudakov double logarithms in their perturbative expansion. Such observables are purely single logarithmic, i.e. the dominant tower of logarithmic corrections are of the form $\alpha_s^n L^n$. Correspondingly, the precise form of the upper kinematic bound on the emission's rapidity (2.16) is irrelevant in the resummation of such observables, and it can be relaxed and replaced by a finite (albeit sufficiently large) rapidity buffer for the radiation within each emitting dipole.

For observables with a double logarithmic perturbative expansion, the resummation presented here must be supplemented with the correct resummation of the corresponding collinear logarithms (obtained with standard techniques for global observables), and the double counting between the two regions (i.e. the soft and collinear limit) must be consistently subtracted. We do not address this subtraction in the present article.

3 Integral equations and the generating functional method

In this article we wish to formulate a solution to the above integro-differential equations in terms of an algorithmic procedure. Moreover, while the above equations have been derived for the family of additive observables, the dynamics they describe is completely general and governs the resummation of non-global QCD corrections in more generic cases. As a first step, we therefore wish to re-write the evolution equations using a language that makes them suitable for: *i)* a numerical implementation via a Monte-Carlo algorithm; *ii)* the application to a generic non-global observable sensitive to soft radiation at large angles.

To carry out this extension, we reinterpret the evolution equations given in the previous section by exploiting a theoretical tool that has been widely used in the area of jet calculus, the generating functional method [49–51].

JHEP03(2022)135

We reinterpret the source $u(k)$ as a *probing function*, whose role is to assign a tag to a real emission k. The probability associated with a state of n real partons $dP_n^{\{12\}}$ produced within a dipole $\{12\}$ is then defined by the following functional derivative

$$dP_n^{\{12\}} = \mathcal{C}(n) \left(\prod_{i=1}^{n} [dk_i] \frac{\delta}{\delta u(k_i)} \right) Z_{12}[Q;\{u\}] \Big|_{\{u\}=0} , \tag{3.1}$$

where the action of the functional derivative on $Z_{12}[Q;\{u\}]$ is defined by

$$\frac{\delta}{\delta u(k_i)} u(k) := \bar{\delta}(k - k_i) = 2(2\pi)^{3-2\epsilon} \delta^{(2-2\epsilon)}(\vec{k}_t - \vec{k}_{ti}) \delta(\eta - \eta_i), \tag{3.2}$$

with the transverse momentum $\vec{k}_{ti}$ and rapidity η_i being defined w.r.t. the emitting colour dipole. The quantity $\mathcal{C}(n)$ is an appropriate combinatorial factor for a state with n (not necessarily identical) particles. For identical particles one simply has $\mathcal{C}(n) = 1/n!$. The above equation defines the *generating* functional $Z_{12}[Q;\{u\}]$, whose probabilistic interpretation (3.1) is crucial to derive a Monte-Carlo procedure for its calculation.

We can now reinterpret the factorisation of the NLL cumulative cross section (2.3) for an observable $V(\{k_i\}) < v$ in terms of generating functionals simply by summing over all possible configurations

$$\begin{aligned} \Sigma(v) = \mathcal{H}_2 \otimes \left[\sum_{i=0}^{\infty} \int dP_i^{\{12\}} \Theta(v - V(\{k_i\})) \right] \\ + \mathcal{H}_3 \otimes \left[\left(\sum_{i=0}^{\infty} \int dP_i^{\{13\}} \right) \left(\sum_{j=0}^{\infty} \int dP_j^{\{23\}} \right) \Theta(v - V(\{k_i\},\{k_j\})) \right] + \mathcal{O}(\text{NNLL}) , \end{aligned} \tag{3.3}$$

where the zero-th terms of the above sums reduce to the pure no-emission probability (i.e. a Sudakov factor), whose perturbative expansion starts with $1 + \mathcal{O}(\alpha_s)$. To calculate the above probabilities, we observe that the generating functional $Z_{12}[Q;\{u\}]$ satisfies the same evolution equations as the Laplace transform of the soft factor (2.12) with the same boundary conditions and with the source $u(k)$ now playing the role of the probing function. In the case of the generating functional, it is more convenient to recast these equations in integral form which, as we will see shortly, offers a simple probabilistic interpretation that can be exploited to construct a Monte Carlo procedure to calculate their solution. Following the derivation in section 4 of ref. [16], we introduce the NLL Sudakov form factor associated with the no-emission probability within the dipole $\{12\}$

$$\ln \Delta_{12}(Q) = - \int [dk] \Theta(Q - k_t) \bar{\alpha}(k_t) w_{12}^{(0)}(k) \left(1 + \bar{\alpha}(k_t) \bar{K}^{(1)} \right) , \tag{3.4}$$

and we take the $\ln Q$ derivative of $Z_{12}[Q;\{u\}]/\Delta_{12}(Q)$

$$Q\partial_Q \frac{Z_{12}[Q;\{u\}]}{\Delta_{12}(Q)} = \frac{\mathbb{K}[Z[Q;\{u\}],u]}{\Delta_{12}(Q)} - Z_{12}[Q;\{u\}] \frac{Q\partial_Q \Delta_{12}(Q)}{\Delta_{12}^2(Q)} . \tag{3.5}$$

JHEP03(2022)135

Using the NLL kernel (2.19) and (3.4) in the above equation, and integrating over $\ln Q$ with the boundary condition (2.30) for Z_{12} leads to the integral equation [16]

$$Z_{12}[Q;\{u\}] = \mathbb{K}_{\rm int}^{\rm RV+VV}[Z[Q;u],u] + \mathbb{K}_{\rm int}^{\rm RR}[Z[Q;u],u] - \mathbb{K}_{\rm int}^{\rm DC}[Z[Q;u],u]\,, \tag{3.6}$$

where we have defined the *integrated* kernels as

$$\begin{aligned}
\mathbb{K}_{\rm int}^{\rm RV+VV}[Z[Q;u],u] &= \Delta_{12}(Q) + \int [dk_a]\bar{\alpha}(k_{ta}) w_{12}^{(0)}(k_a) \left(1 + \bar{\alpha}(k_{ta})\,\bar{K}^{(1)}\right) \frac{\Delta_{12}(Q)}{\Delta_{12}(k_{ta})} \\
&\quad \times Z_{1a}[k_{ta};\{u\}] Z_{a2}[k_{ta};\{u\}] u(k_a) \Theta(Q - k_{ta})\,,
\end{aligned} \tag{3.7}$$

$$\begin{aligned}
\mathbb{K}_{\rm int}^{\rm RR}[Z[Q;u],u] &= \int [dk_a] \int [dk_b]\, \bar{\alpha}^2(k_{t(ab)}) \Theta(Q - k_{t(ab)}) \Theta(k_{ta} - k'_{tb}) \frac{\Delta_{12}(Q)}{\Delta_{12}(k_{t(ab)})} \\
&\quad \times \Big[\bar{w}_{12}^{(gg)}(k_b,k_a) Z_{1b}[k_{t(ab)};\{u\}] Z_{ba}[k_{t(ab)};\{u\}] Z_{a2}[k_{t(ab)};\{u\}] u(k_a) u(k_b) \\
&\quad + \bar{w}_{12}^{(gg)}(k_a,k_b) Z_{1a}[k_{t(ab)};\{u\}] Z_{ab}[k_{t(ab)};\{u\}] Z_{b2}[k_{t(ab)};\{u\}] u(k_a) u(k_b) \\
&\quad - \left(\bar{w}_{12}^{(gg)}(k_b,k_a) + \bar{w}_{12}^{(gg)}(k_a,k_b) \right) Z_{1(ab)}[k_{t(ab)};\{u\}] Z_{(ab)2}[k_{t(ab)};\{u\}] u(k_{(ab)}) \Big]\,,
\end{aligned} \tag{3.8}$$

$$\begin{aligned}
\mathbb{K}_{\rm int}^{\rm DC}[Z[Q;u],u] &= \int [dk_a] \int [dk_b] \bar{\alpha}^2(k_{ta}) \Theta(Q - k_{ta}) \Theta(k_{ta} - k_{tb}) \frac{\Delta_{12}(Q)}{\Delta_{12}(k_{ta})} \\
&\quad \times \Big[w_{12}^{(0)}(k_a) \left(w_{1a}^{(0)}(k_b) - \frac{1}{2} w_{12}^{(0)}(k_b) \right) Z_{1b}[k_{ta};\{u\}] Z_{ba}[k_{ta};\{u\}] Z_{a2}[k_{ta};\{u\}] u(k_a) u(k_b) \\
&\quad + w_{12}^{(0)}(k_a) \left(w_{a2}^{(0)}(k_b) - \frac{1}{2} w_{12}^{(0)}(k_b) \right) Z_{1a}[k_{ta};\{u\}] Z_{ab}[k_{ta};\{u\}] Z_{b2}[k_{ta};\{u\}] u(k_a) u(k_b) \\
&\quad - w_{12}^{(0)}(k_a) \left(w_{1a}^{(0)}(k_b) + w_{a2}^{(0)}(k_b) - w_{12}^{(0)}(k_b) \right) Z_{1a}[k_{ta};\{u\}] Z_{a2}[k_{ta};\{u\}] u(k_a) \Big]\,.
\end{aligned} \tag{3.9}$$

Eq. (3.6) defines the NLL generating functional for the non-global evolution. At NLL, at most one gluon at a time inside the interjet rapidity gap is considered in eqs. (3.8), (3.9), with configurations with multiple gluons giving rise to at most NNLL corrections. This constraint is implicitly enforced in all evolution equations (2.12) and (3.6) given up to this point. When taking the four-dimensional limit, one has to supplement eq. (3.6) with a non-perturbative prescription to regulate the Landau singularity. We will assume eq. (2.31), which will be understood in the following, but alternative models can be adopted.

At LL accuracy, the evolution equation for the generating functional (3.6) is drastically simplified and it becomes

$$\begin{aligned}
Z_{12}[Q;\{u\}] &= \Delta_{12}(Q) + \int [dk_a] \bar{\alpha}(k_{ta}) w_{12}^{(0)}(k_a) \frac{\Delta_{12}(Q)}{\Delta_{12}(k_{ta})} \\
&\quad \times Z_{1a}[k_{ta};\{u\}] Z_{a2}[k_{ta};\{u\}] u(k_a) \Theta(Q - k_{ta})\,,
\end{aligned} \tag{3.10}$$

with the LL Sudakov form factor given by

$$\ln \Delta_{12}(Q) = -\int [dk] \Theta(Q - k_t) \bar{\alpha}(k_t) w_{12}^{(0)}(k)\,. \tag{3.11}$$

If we set $u = 0$ in eq. (3.10), the functional $Z_{12}[Q;\{u\}]$ gives the probability of having no emissions from the dipole $\{12\}$ which, as anticipated after eq. (3.3), coincides with the Sudakov form factor.

JHEP03(2022)135

Before introducing an algorithmic solution of eqs. (3.6), (3.10), we make some considerations that will be exploited in their numerical implementation. We start by considering the term proportional to the independent emission squared amplitude $w_{12}^{(0)}(k_a)w_{12}^{(0)}(k_b)$ in eqs. (3.9) and (3.8). According to eq. (2.28) the dipole transverse momentum k_{tb} in this term is meant to be relative to the $\{12\}$ dipole, i.e. $k_{tb} = k'_{tb}$ by definition for this contribution. We now express $\bar{w}_{12}^{(gg)}$ in (3.8) according to its definition eq. (2.25) and we consider the terms in $\mathbb{K}_{\text{int}}^{\text{RR}}$ containing $w_{12}^{(0)}(k_a)w_{12}^{(0)}(k_b)$, namely (with $k_{tb} = k'_{tb}$)

$$\begin{aligned}
\mathbb{K}_{\text{int}}^{\text{RR, indep.}}[Z[Q;u],u] = &-\int [dk_a]\int [dk_b]\,\bar{\alpha}^2(k_{t(ab)})\Theta(Q-k_{t(ab)})\Theta(k_{ta}-k_{tb})\frac{\Delta_{12}(Q)}{\Delta_{12}(k_{t(ab)})} \\
&\times w_{12}^{(0)}(k_a)w_{12}^{(0)}(k_b)\bigg[\frac{1}{2}Z_{1b}[k_{t(ab)};\{u\}]Z_{ba}[k_{t(ab)};\{u\}]Z_{a2}[k_{t(ab)};\{u\}]u(k_a)u(k_b) \\
&+\frac{1}{2}Z_{1a}[k_{t(ab)};\{u\}]Z_{ab}[k_{t(ab)};\{u\}]Z_{b2}[k_{t(ab)};\{u\}]u(k_a)u(k_b) \\
&- Z_{1(ab)}[k_{t(ab)};\{u\}]Z_{(ab)2}[k_{t(ab)};\{u\}]u(k_{(ab)})\bigg]\,.
\end{aligned} \tag{3.12}$$

We observe that the difference between the above equation and the corresponding term proportional to $w_{12}^{(0)}(k_a)w_{12}^{(0)}(k_b)$ in eq. (3.9) is logarithmically subleading, contributing at most a NNLL correction. That is to say that the emission of independent soft gluons is already correctly iterated by eq. (3.7) in the kinematic regime that is relevant to NLL. This can be understood from simple power counting arguments. Let us first consider the difference between the double real contributions, i.e. those proportional to the product of two probing functions $u(k_a)u(k_b)$. Unlike the rest of the double real corrections in eqs. (3.8), (3.9) this term is infrared finite and it is non-zero only if the two emissions have commensurate transverse momenta in the $\{12\}$ dipole frame. This condition, together with the fact that the observable is insensitive to the region in which k_a and k_b are collinear to the $\{12\}$ dipole extremities implies that this term yields a relative $\mathcal{O}(\bar{\alpha}^2)$ correction to the integral equation with no further logarithmic enhancement, that is NNLL. Analogous considerations hold for the difference between the collinear counter-terms in eqs. (3.9), (3.12), and allow us to conclude that all terms proportional to $w_{12}^{(0)}(k_a)w_{12}^{(0)}(k_b)$ in the r.h.s. of eq. (3.6) can be neglected for the observables under consideration.

We now observe that the integrated kernel $\mathbb{K}_{\text{int}}^{\text{RV+VV}}[Z[Q;u],u]$ in eq. (3.6) has the same functional form as the LL equation (3.10), and it can be solved with the same algorithm (Algorithm 1 in section 4). It is therefore appropriate to split $Z_{12}[Q;\{u\}]$ into the sum of two contributions as[3]

$$Z_{12}[Q;\{u\}] = Z_{12}^{(0)}[Q;\{u\}] + Z_{12}^{(1)}[Q;\{u\}]\,, \tag{3.13}$$

where $Z_{12}^{(0)}[Q;\{u\}]$ satisfies the integral equation

$$\begin{aligned}
Z_{12}^{(0)}[Q;\{u\}] = \Delta_{12}(Q) + &\int [dk_a]\bar{\alpha}(k_{ta})w_{12}^{(0)}(k_a)\left(1+\bar{\alpha}(k_{ta})\,\bar{K}^{(1)}\right)\frac{\Delta_{12}(Q)}{\Delta_{12}(k_{ta})} \\
&\times Z_{1a}^{(0)}[k_{ta};\{u\}]Z_{a2}^{(0)}[k_{ta};\{u\}]u(k_a)\Theta(Q-k_{ta})\,,
\end{aligned} \tag{3.14}$$

[3]The strategy that follows is inspired to what has been already applied to the NNLL calculation of global QCD observables [54–58], and specifically to the insertion of a *correlated* pair of soft partons.

JHEP03(2022)135

with Δ_{12} defined in eq. (3.4). We can now treat $Z_{12}^{(1)}[Q;\{u\}]$ as a perturbation, observing that all contributions to $\Sigma(v)$ that are quadratic in $Z_{12}^{(1)}[Q;\{u\}]$ (as well as those proportional to $Z_{12}^{(1)}[Q;\{u\}]\bar{K}^{(1)}$) only correspond to NNLL corrections. We can therefore linearise eq. (3.6) in $Z_{12}^{(1)}[Q;\{u\}]$ by inserting eq. (3.13) into eq. (3.6) and neglecting the aforementioned quadratic corrections:

$$
\begin{aligned}
Z_{12}^{(1)}[Q;\{u\}] \simeq & \int [dk_a] \bar{\alpha}(k_{ta}) w_{12}^{(0)}(k_a) \, \frac{\Delta_{12}(Q)}{\Delta_{12}(k_{ta})} \\
& \times \left(Z_{1a}^{(0)}[k_{ta};\{u\}] Z_{a2}^{(1)}[k_{ta};\{u\}] + Z_{1a}^{(1)}[k_{ta};\{u\}] Z_{a2}^{(0)}[k_{ta};\{u\}] \right) u(k_a) \Theta(Q - k_{ta}) \\
& + \int [dk_a] \int [dk_b] \, \bar{\alpha}^2(k_{t(ab)}) \Theta(Q - k_{t(ab)}) \Theta(k_{ta} - k'_{tb}) \frac{\Delta_{12}(Q)}{\Delta_{12}(k_{t(ab)})} \\
& \times \Big[\tilde{w}_{12}^{(0)}(k_b, k_a) Z_{1b}^{(0)}[k_{t(ab)};\{u\}] Z_{ba}^{(0)}[k_{t(ab)};\{u\}] Z_{a2}^{(0)}[k_{t(ab)};\{u\}] u(k_a) u(k_b) \\
& + \tilde{w}_{12}^{(0)}(k_a, k_b) Z_{1a}^{(0)}[k_{t(ab)};\{u\}] Z_{ab}^{(0)}[k_{t(ab)};\{u\}] Z_{b2}^{(0)}[k_{t(ab)};\{u\}] u(k_a) u(k_b) \\
& - \left(\tilde{w}_{12}^{(0)}(k_b, k_a) + \tilde{w}_{12}^{(0)}(k_a, k_b) \right) Z_{1(ab)}^{(0)}[k_{t(ab)};\{u\}] Z_{(ab)2}^{(0)}[k_{t(ab)};\{u\}] u(k_{(ab)}) \Big] \\
& - \int [dk_a] \int [dk_b] \bar{\alpha}^2(k_{ta}) \Theta(Q - k_{ta}) \Theta(k_{ta} - k_{tb}) \frac{\Delta_{12}(Q)}{\Delta_{12}(k_{ta})} \\
& \times \Big[w_{12}^{(0)}(k_a) w_{1a}^{(0)}(k_b) Z_{1b}^{(0)}[k_{ta};\{u\}] Z_{ba}^{(0)}[k_{ta};\{u\}] Z_{a2}^{(0)}[k_{ta};\{u\}] u(k_a) u(k_b) \\
& + w_{12}^{(0)}(k_a) w_{a2}^{(0)}(k_b) Z_{1a}^{(0)}[k_{ta};\{u\}] Z_{ab}^{(0)}[k_{ta};\{u\}] Z_{b2}^{(0)}[k_{ta};\{u\}] u(k_a) u(k_b) \\
& - w_{12}^{(0)}(k_a) \left(w_{1a}^{(0)}(k_b) + w_{a2}^{(0)}(k_b) \right) Z_{1a}^{(0)}[k_{ta};\{u\}] Z_{a2}^{(0)}[k_{ta};\{u\}] u(k_a) \Big] ,
\end{aligned}
\tag{3.15}
$$

where $\simeq$ indicates that we neglect corrections of order NNLL and higher. Eq. (3.15) has a simple physical interpretation. The two double integrals in the r.h.s. of eq. (3.15) correspond to an *insertion* of a pair of soft gluons k_a, k_b with commensurate energies (or transverse momenta in the $\{12\}$ frame), but strongly ordered w.r.t. the rest of the soft radiation in the evolution. The emission of the unordered pair will give rise to three colour dipoles (two for the corresponding collinear counter-terms), which will subsequently evolve according to the evolution equation (3.14). The first term in the r.h.s. of eq. (3.15) states that such insertion can occur at *any* stage of the evolution, i.e. the pair k_a, k_b does not necessarily correspond to the first two soft gluons emitted off the initial $q\bar{q}$ dipole. This structure is depicted in the evolution tree of figure 2, where the edges of the graph correspond to colour dipoles. In this example, each node corresponds to the splitting of a dipole into two adjacent dipoles according to eq. (3.14), with the exception of the (red) splitting of the dipole $\{49\}$ which depicts the double emission insertion in the r.h.s. of eq. (3.15). This $Z^{(1)}[Q;\{u\}]$ insertion can occur at any branching, and one needs therefore to sum over all possible configurations. This procedure is a perturbative solution of eq. (3.6), where we neglect corrections that are subleading (i.e. NNLL) in the strict logarithmic counting. One could also envision an algorithmic solution of the full integral equation, in which roughly speaking the insertion of $Z^{(1)}[Q;\{u\}]$ is iterated an arbitrary number of times. The corresponding algorithm would differ from the solution presented here by NNLL corrections, and it would be directly relevant for the inclusion of NLL non-global corrections in the

JHEP03(2022)135

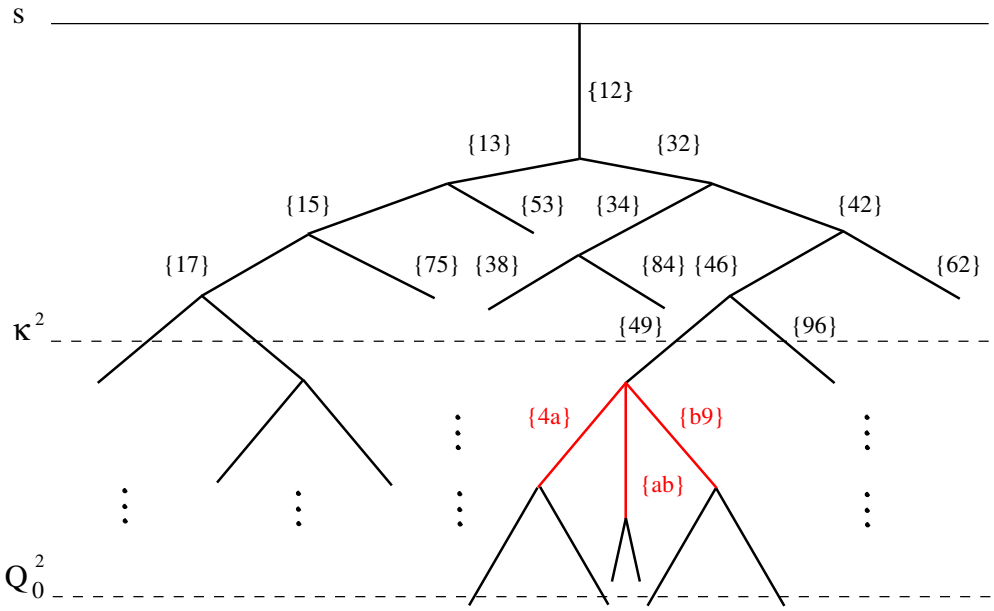

Figure 2. Example of an evolution tree of dipole $\{12\}$. Each edge in the graph corresponds to a dipole. The nodes correspond to an iteration of $Z^{(0)}[Q;\{u\}]$ except for the (red) node describing the splitting of dipole $\{49\}$ which indicates the double emission insertion in the r.h.s. of the evolution equation (3.15) for $Z^{(1)}[Q;\{u\}]$.

frame of a full-fledged dipole shower. For this reason, its formulation is left for future investigations.

The above equations can be solved recursively, for which Monte Carlo techniques offer a natural theoretical tool. In the next section we will introduce the necessary algorithms to perform the NLL resummation using the technology of dipole showers ordered in the dipole transverse momentum. Algorithms of this type are very common in the parton shower literature (see e.g. refs. [39, 40, 59–63]), and at present they usually achieve LL accuracy for the observables considered in this article. Notice, however, that in the present paper these Monte Carlo techniques are simply used to solve numerically the evolution equations and not to build an actual generator of physical events.

4 Perturbative solution of the evolution equations

In this section we discuss how eq. (3.3) can be calculated using Monte Carlo methods. We will start with section 4.1 by reporting the dipole-shower algorithm to solve the LL counter-part of eq. (3.6), originally derived in ref. [1], then we move on to discuss the NLL corrections to the cumulative cross section (2.3) (or equivalently (3.3)), in configurations with three (section 4.2) and two (section 4.3) hard partons in the final state.

In the rest of this article, we also restore the full dependence on N_c both in the QCD beta function used in the evolution of the running coupling (2.17) and in the cusp anomalous

JHEP03(2022)135

dimension (2.21). This by no means implies full control over finite-N_c corrections, as additional subleading-N_c terms are neglected in the evolution equations. We therefore replace eq. (2.17) with the full RGE (notice that an overall factor N_c/π is present in eq. (2.17))

$$\frac{d\alpha_s(\mu)}{d\ln\mu^2} = -\beta(\alpha_s) = -\alpha_s\left(\beta_0\alpha_s + \beta_1\alpha_s^2 + \dots\right), \tag{4.1}$$

with

$$\beta_0 = \frac{11C_A - 2n_F}{12\pi}, \quad \beta_1 = \frac{17C_A^2 - 5C_An_F - 3C_Fn_F}{24\pi^2}. \tag{4.2}$$

Moreover we replace in eq. (3.6)

$$\bar{\alpha}(k_{ta})\bar{K}^{(1)} \to \frac{\alpha_s(k_{ta})}{2\pi}K^{(1)}, \quad K^{(1)} = \left(\frac{67}{18} - \frac{\pi^2}{6}\right)C_A - \frac{5}{9}n_F. \tag{4.3}$$

Similarly, we will retain the full colour quadratic SU(N_c) Casimir operators in the calculation of the hard coefficients $\mathcal{H}_2$ and $\mathcal{H}_3$ in section 4.2 below.

4.1 LL evolution algorithm

At LL, eq. (3.10) can be solved with the dipole shower algorithm derived in the pioneering article by Dasgupta and Salam [1], that we adapt below to the problem considered here and to the case of dipole-transverse-momentum ordering. For later use, we define the *evolution time*

$$t \coloneqq \int_{\frac{k_t}{\sqrt{s}}}^{1}\frac{dx}{x}\bar{\alpha}(x\sqrt{s}) = -\frac{N_c}{2\pi\beta_0}\ln\left(1-2\lambda\right), \qquad \lambda = \beta_0\alpha_s(\sqrt{s})\ln\frac{\sqrt{s}}{k_t}. \tag{4.4}$$

The solution to eq. (3.10) is then obtained with Algorithm 1, which is iterated until the desired statistical precision is reached. In the following, we define the infrared scale Q_0 as the singularity of eq. (4.4), namely such that

$$2\,\beta_0\alpha_s(\sqrt{s})\ln\frac{\sqrt{s}}{Q_0} = 1. \tag{4.5}$$

In practice, this scale is extremely low and therefore the evolution is rarely stopped because the scale Q_0 is reached before any emission is radiated into the interjet rapidity gap.

An important aspect to stress about Algorithm 1, is that at every step emissions are generated in the emitting dipole rest frame, but the observable is calculated in the event frame. We therefore need to apply a simple Lorentz transformation at every evolution step to transform the generated emission into the event frame. In doing this, we only need to keep track of the direction of the generated momenta, while the information regarding the *dipole* transverse momentum (i.e. the normalisation of the momenta) is encoded in the evolution time t. Therefore, we divide all momenta by their energy in the event frame, and keep track of the normalisation separately. As in ref. [1], all Lorentz transformations discussed in all algorithms presented in this section have to be performed with *normalised* momenta. This solves the problem of handling numerically Lorentz transformations involving very soft momenta. Also, it allows us to perform the evolution without any momentum

JHEP03(2022)135

Algorithm 1: LL evolution algorithm

Set $i = 0$ and the evolution time $t_0 = 0$;
Start with one initial dipole made by the Born fermionic line;
while true **do**
  Compute $\Delta\eta_{\rm tot} = \sum_{\ell=1}^{N} \Delta\eta_\ell$, the sum of the available rapidity ranges within each of the N dipoles in the event so far;
  Increase i by 1;
  Generate a random number $r \in [0,1]$ & increase t by an amount $\Delta t = t_i - t_{i-1}$ generated by solving

$$\frac{\Delta_{12}(k_{t,i-1})}{\Delta_{12}(k_{t,i})} = e^{-\Delta\eta_{\rm tot}\Delta t} = r\,;$$

  Generate the *dipole* transverse momentum $k_{t,i}$ of the next emission k_i by solving eq. (4.4) with the new t_i. Generate its azimuth uniformly in $[0, 2\pi]$ and its rapidity such that the magnitude of the rapidity with respect to the dipole extremities in the *event* frame is less than δ, as done in ref. [1];
  Choose the emitting dipole $\mathcal{D}_\ell$ with probability $\Delta\eta_\ell/\Delta\eta_{\rm tot}$;
  if $k_{t,i} < Q_0$ **then**
    break;
  end
  Split the dipole $\mathcal{D}_\ell$ into two adjacent dipoles;
  if $\Theta_{\rm in}(k_i) = 1$ **then**
    Calculate observable and add the event to the histogram & break;
  end
end

conservation at any evolution step, thus eliminating exactly all subleading power (i.e. non-logarithmic) corrections. We now discuss the calculation of the observable in a given event. The evolution in Algorithm 1 stops as soon as one gluon is emitted inside the interjet rapidity gap. We then calculate the transverse energy E_t of this gluon w.r.t. the thrust axis of the event, and add the event to the histogram. We notice that in ref. [2], the transverse energy is instead defined as the value of the ordering variable. This definition is correct at LL, but the exact relation between the ordering variable and the actual observable leads to a genuine NLL effect. In this article we include these effects already in the LL prediction, and therefore we work with the physical observable everywhere in our calculation.

4.2 NLL evolution algorithm: $\mathcal{H}_3 \otimes S_3(v)$ contribution

We now move on with the NLL corrections. We start from the $\mathcal{H}_3 \otimes S_3(v)$ contribution to the cumulative cross section (2.3), which describes the production of three hard partons inside the jets (i.e. outside the interjet rapidity gap). The three partons can be viewed as two independent colour dipoles in a large-N_c picture (in the case of e^+e^- collisions), labelled as $\{13\}$ and $\{23\}$ in the second term of the r.h.s. of eq. (3.3). These subsequently emit soft

JHEP03(2022)135

radiation independently of each other into the measured interjet region. The soft evolution of each of the above two dipoles, encoded in S_3, is carried out at LL order using Algorithm 1, and it is therefore straightforward. However, some care must be taken in the calculation of the hard factor $\mathcal{H}_3$ corresponding to the three hard-parton contribution. Specifically, in ref. [16] as well as in section 2 we have stated that the hard factors are individually IRC finite, while the integral over the three-parton final state clearly has divergences associated to singular kinematic configurations. At NLL, these divergences are meant to be cancelled by corresponding divergent contributions in the virtual corrections entering $\mathcal{H}_2$, and such a cancellation has to be enforced by means of a subtraction procedure. This also implies that the precise definition of the hard matching coefficients $\mathcal{H}_2$ and $\mathcal{H}_3$ depends on the scheme adopted to subtract their IRC divergences and only their combination has a physical meaning. In section 5 of ref. [16] the calculation was carried out analytically. However, in this article we would like to take a different approach and set up a numerical calculation using a local subtraction method that can be easily applied to the case of more complicated processes. As a consequence, the individual definition of $\mathcal{H}_2$ and $\mathcal{H}_3$ computed here will differ from those of ref. [16] while their physical sum will be identical.

We start by labelling with p_1, p_2, p_3 the quark, antiquark and gluon respectively. With the usual x_1, x_2, x_3 variables

$$x_i = \frac{2(p_i \cdot q)}{s}\,, \quad i = 1,2,3\,, \qquad x_1 + x_2 + x_3 = 2\,, \tag{4.6}$$

where q is the four momentum of the virtual photon $q^\mu = (\sqrt{s}, \vec{0})$. To obtain $\mathcal{H}_3 \otimes S_3(v)$, we start by evaluating the integral over the $q\bar{q}g$ phase space. We choose the reference frame so that the z axis is along the direction of the quark $\vec{p}_1$, and we explicitly parametrise the phase space of the remaining two partons in terms of the energy fraction of the gluon $x_3 = 2E_g/\sqrt{s}$ and the cosine of the angle between the gluon and the quark $y = \cos\theta_{qg}$. The real contribution to $\mathcal{H}_3 \otimes S_3(v)$ is

$$\begin{aligned}\Sigma^{\text{real}}(v) = 2C_F \frac{\alpha_s}{2\pi}\left(\frac{\mu^2}{s}\right)^{\epsilon} \frac{e^{\gamma_E \epsilon}}{\Gamma(1-\epsilon)} \int_0^1 dx_3 \frac{x_3^{-1-2\epsilon}}{(1-x_3)^{2\epsilon}} \int_{-1}^1 dy \frac{(1-y)^{-1-\epsilon}(1+y)^{-1-\epsilon}}{(2-x_3(1-y))^{2-2\epsilon}} \\ \times \Big(8 - \epsilon x_3^2 (2 - x_3(1-y))^2 - (2-x_3)x_3\Big((x_3-2)x_3(1-y)^2 - 4y + 8\Big)\Big) \\ \times \Theta_{\text{out}}(p_1)\Theta_{\text{out}}(p_2)\Theta_{\text{out}}(p_3)\, S_3(v)\,,\end{aligned} \tag{4.7}$$

where the coupling has been renormalised in the $\overline{\text{MS}}$ scheme. The phase space constraint $\Theta_{\text{out}}(p_1)\Theta_{\text{out}}(p_2)\Theta_{\text{out}}(p_3)$ is non trivial, and imposes that none of the hard particles ends up inside the interjet rapidity gap, as per definition of $\mathcal{H}_3$. We stress that the direction of the thrust axis, that is used to define the position of the interjet rapidity gap, is now aligned with the hardest parton. For a given value of x_3 and y the event is then dressed by a shower of soft gluons encoded in S_3, so that the integration over the remaining phase space of the three-parton system (specifically y) involves also the soft factor S_3. Eq. (4.7) produces double and single poles of soft and collinear origin, and we wish to perform a local subtraction of these divergences so that the above integral is computed numerically. We consider a simple subtraction scheme in which the local counter-term is defined by the

JHEP03(2022)135

full real integrand albeit with unresolved kinematics. That is, we build the counter-term by replacing the phase space constraint in eq. (4.7) with

$$\Theta_{\text{out}}(p_1)\Theta_{\text{out}}(p_2)\Theta_{\text{out}}(p_3) \to \Theta^{\text{soft}}_{\text{out}}(p_3)\,. \tag{4.8}$$

Here $\Theta^{\text{soft}}_{\text{out}}(p_3)$ indicates that when the gluon p_3 is unresolved (i.e. either soft or collinear to either quark leg) the thrust axis is aligned along the z-axis and therefore $\Theta_{\text{out}}(p_1) = \Theta_{\text{out}}(p_2) = 1$ by construction. The addition of such a counter-term modifies eq. (4.7) as follows

$$\begin{aligned}\Sigma^{(3),\text{sub}}(v) = 2C_F\frac{\alpha_s}{2\pi}\left(\frac{\mu^2}{s}\right)^{\epsilon}\frac{e^{\gamma_E\epsilon}}{\Gamma(1-\epsilon)}\int_0^1 dx_3\frac{x_3^{-1-2\epsilon}}{(1-x_3)^{2\epsilon}}\int_{-1}^1 dy\,\frac{(1-y)^{-1-\epsilon}(1+y)^{-1-\epsilon}}{(2-x_3(1-y))^{2-2\epsilon}}\\ \times\Big(8-\epsilon x_3^2(2-x_3(1-y))^2-(2-x_3)x_3\Big((x_3-2)x_3(1-y)^2-4y+8\Big)\Big)\\ \times\Big[\Theta_{\text{out}}(p_1)\Theta_{\text{out}}(p_2)\Theta_{\text{out}}(p_3)\,S_3(v)-\Theta^{\text{soft}}_{\text{out}}(p_3)\,S_2(v)\Big]\,,\end{aligned} \tag{4.9}$$

where S_2 in the last term indicates that the soft factor now does not see the unresolved gluon p_3 and therefore it degenerates into the two-leg factor S_2. We point out that this procedure is a simple adaptation of the *projection-to-Born* subtraction method [64] to an all-order calculation, where the projection acts on the full real phase space including the soft factor S_3. Eq. (4.9) is free of collinear singularities, however it still contains a soft singularity due to the fact that $S_3(v)$ depends on the direction of p_3 regardless of how soft the latter is. We then introduce a technical cutoff on the transverse momentum of the gluon p_3 w.r.t. the $\{12\}$ dipole ($p_{t,3}^{\{12\}} > Q_0$), and we set $\epsilon \to 0$ and evaluate the integral with Algorithm 2 (again iterated until the desired statistical precision is reached). The computation of eq. (4.9) does not directly return the contribution $\mathcal{H}_3 \otimes S_3(v)$. This is obtained by subtracting the double counting with the term $\mathcal{H}_2 \otimes S_2(v)$, where the first gluon p_3 is now generated according to the LL evolution kernel. This requires subtracting from eq. (4.9) the term [16] (we set $N_c \to 2C_F$ for this first emission)

$$\Sigma^{(3),\text{sub}}_{\text{soft}}(v) = 4C_F\frac{\alpha_s}{2\pi}\mu^{2\epsilon}\frac{e^{\gamma_E\epsilon}}{\Gamma(1-\epsilon)}\int_0^{\sqrt{s}}\frac{dk_t}{k_t^{1+2\epsilon}}\int_{\ln(k_t/\sqrt{s})}^{\ln(\sqrt{s}/k_t)}d\eta\,\Theta^{\text{soft}}_{\text{out}}(k)\left[S_3^{\text{soft}}(v)-S_2(v)\right]\,, \tag{4.10}$$

where S_3^{soft} indicates that the emission of the soft gluon k does not cause any recoil in the $q\bar{q}g$ event kinematics, and therefore the thrust axis is always aligned with the z-axis. In eq. (4.10) we have adopted the same subtraction method used in eq. (4.9), thereby subtracting the local counter-term evaluated in the unresolved (i.e. two-leg) kinematics. Eq. (4.10) also contains the soft singularity present in eq. (4.9), and therefore we need to apply the same technical cutoff $k_t > Q_0$ here. It is now crucial to notice that the difference between the two equations is instead finite in the limit $Q_0 \to 0$, and the regulator can be pushed to negligibly small values in the combination of the two. Eq. (4.10) can be evaluated with a slightly modified version of Algorithm 2, given in Algorithm 3. Finally we obtain $\mathcal{H}_3 \otimes S_3(v)$ as the *difference* between the two contributions

$$\mathcal{H}_3 \otimes S_3(v) = \Sigma^{(3),\text{sub}}(v) - \Sigma^{(3),\text{sub}}_{\text{soft}}(v)\,. \tag{4.11}$$

JHEP03(2022)135

Algorithm 2: NLL evolution algorithm for $\mathcal{H}_3 \otimes S_3(v)$

Generate x_3 and y and parametrise the kinematics of the $q\bar{q}g$ system in terms of these variables;
if $p_{t,3}^{\{12\}} < Q_0$ **then**
  break and generate a new event;
end
Set the weight w to the integrand in the first two lines of eq. (4.9) with $\epsilon = 0$;
Create an *event*:
while true **do**
  Set the thrust axis along the direction of the hardest parton;
  if $\Theta_{\rm out}(p_1)\Theta_{\rm out}(p_2)\Theta_{\rm out}(p_3) = 0$ **then**
    break;
  end
  Consider the two large-N_c dipoles $\{13\}$ and $\{23\}$ and apply the LL evolution algorithm 1 to compute the soft factor S_3 at leading colour;
  break;
end
Create a *counter-event*:
Set $w *= -1$;
while true **do**
  Set the thrust axis along the direction of the quark (z direction);
  if $\Theta_{\rm out}^{\rm soft}(p_3) = 0$ **then**
    break;
  end
  Consider the dipole $\{12\}$ and apply the LL evolution algorithm 1 to compute the soft factor S_2 while filling the same histogram as for the event;
  break;
end

The above procedure used to define $\mathcal{H}_3$ implicitly also defines uniquely the two-parton hard coefficient $\mathcal{H}_2$. This will be given by the one loop correction to the quark form factor minus the integrals of the local counter-terms appearing in eq. (4.11), minus the virtual correction to the evolution kernel that is subtracted to avoid the double counting with S_2 (see section 5 of ref. [16]). The latter contribution to $\mathcal{H}_2 \otimes S_2(v)$ reads [16]

$$\Sigma_{\rm soft}^{(2),\rm virt.}(v) = 4C_F \frac{\alpha_s}{2\pi}\mu^{2\epsilon}\frac{e^{\gamma_E\epsilon}}{\Gamma(1-\epsilon)}\int_0^{\sqrt{s}}\frac{dk_t}{k_t^{1+2\epsilon}}\int_{\ln(k_t/\sqrt{s})}^{\ln(\sqrt{s}/k_t)} d\eta\, S_2(v)\,. \tag{4.12}$$

This yields, neglecting $\mathcal{O}(\alpha_s^2)$ corrections,

$$\mathcal{H}_2 = \delta^{(2)}(\Omega_1 - \Omega_q)\delta^{(2)}(\Omega_2 - \Omega_{\bar{q}})\left(1 + \frac{\alpha_s}{2\pi}\mathcal{H}_2^{(1)}\right), \tag{4.13}$$

JHEP03(2022)135

Algorithm 3: NLL evolution algorithm for the soft contribution to $\mathcal{H}_3 \otimes S_3(v)$

Generate $\vec{k}_t$ and η of the gluon k and the back-to-back $q\bar{q}$ pair along the z axis;
if $k_t < Q_0$ **then**
  break and generate a new event;
end
Set the weight w to the integrand in eq. (4.10) with $\epsilon = 0$ (w/o Θ and S_n factors);
Set the thrust axis along the direction of the quark (z direction);
Create an *event*:
while true **do**
  if $\Theta_{\text{out}}^{\text{soft}}(k) = 0$ **then**
    break;
  end
  Consider the two large-N_c dipoles $\{13\}$ and $\{23\}$ and apply the LL evolution algorithm 1 to compute the soft factor S_3^{soft} at leading-colour;
  break;
end
Create a *counter-event*:
Set $w \mathrel{*}= -1$;
while true **do**
  if $\Theta_{\text{out}}^{\text{soft}}(k) = 0$ **then**
    break;
  end
  Consider the dipole $\{12\}$ and apply the LL evolution algorithm 1 to compute the soft factor S_2 while filling the same histogram as for the event;
  break;
end

where

$$\begin{aligned}\mathcal{H}_2^{(1)} = \frac{C_F}{2\left(1-c^2\right)^2}\Bigg(&4\left(1-c^2\right)^2\left(\mathrm{Li}_2\left(\frac{1+c}{2}\right)-\mathrm{Li}_2\left(\frac{1-c}{2}\right)\right)\\&-2\left(1-c^2\right)^2\log^2(1+c)+16c\left(3+c^2\right)\ln(2)-(1-c^2)(c(16+3c)-3)\\&+2\ln(1-c)\left(-2\left(1+c^4\right)\log(2)-4c\left(3+c^2\right)+\left(1-c^2\right)^2\ln(1-c)\right)\\&+\left(4\left(1+c^4\right)\ln(2)-8c\left(3+c^2\right)\right)\ln(1+c)-4\left(-3c^4+2c^2(9+2\ln(2))+1\right)\tanh^{-1}(c)\Bigg).\end{aligned} \tag{4.14}$$

Here c is the cosine of the jet opening angle, defined in eq. (2.1). This coefficient will be used in the next section for the calculation of the $\mathcal{H}_2 \otimes S_2(v)$ contribution to the NLL cumulative cross section.

JHEP03(2022)135

4.3 NLL evolution algorithm: $\mathcal{H}_2 \otimes S_2(v)$ contribution

We now address the numerical solution to the evolution equations (3.14), (3.15). We start by considering the contribution $Z_{12}^{(0)}[Q;\{u\}]$, defined by the evolution equation (3.14). The solution to eq. (3.14) can be obtained with proper modifications of Algorithm 1. However, while Algorithm 1 can be used to calculate $Z_{12}^{(0)}[Q;\{u\}]$, defined by eq. (3.14), in order to include the contribution from $Z_{12}^{(1)}[Q;\{u\}]$ given in eq. (3.15) we cannot simply run Algorithm 1 down to the infrared scale Q_0. Instead, we first introduce a *truncated* version of Algorithm 1, given in Algorithm 4.

Algorithm 4: Truncated NLL algorithm for the first evolution branch

Set the thrust axis along the z axis;
Generate the truncation scale $\kappa \in [Q_0, \sqrt{s}]$ uniformly according to eq. (4.16);
Set the weight $w = \mathcal{H}_2$ as defined in eq. (4.13);
Apply Algorithm 1 with evolution time (4.15) truncated at $Q_0 = \kappa$;

Firstly, we replace the evolution time (4.4) by its NLL counterpart

$$t := \int_{\frac{k_t}{\sqrt{s}}}^{1} \frac{dx}{x} \bar{\alpha}(x\sqrt{s}) \left(1 + \frac{\alpha_s(x\sqrt{s})}{2\pi} K^{(1)}\right) = -\frac{N_c}{2\pi\beta_0} \ln(1-2\lambda) + \bar{\alpha}(\sqrt{s}) \left[\frac{\lambda}{1-2\lambda}\left(\frac{K^{(1)}}{2\pi\beta_0} - \frac{\beta_1}{\beta_0^2}\right) - \frac{\ln(1-2\lambda)}{1-2\lambda}\frac{\beta_1}{2\beta_0^2}\right] + \mathcal{O}(\text{NNLL})\,. \tag{4.15}$$

The above equation uniquely defines the dipole transverse momentum given the evolution time for a given emission. We now introduce the scale κ at which we truncate a first branch of the evolution carried out according to the equation (3.14). The rationale is to use the simple partition of unity in the evolution sequence

$$1 = \int_{Q_0}^{\sqrt{s}} \frac{d\kappa}{\sqrt{s} - Q_0}\,, \tag{4.16}$$

and use the fact that the evolution (3.14) between $\sqrt{s}$ and Q_0 is identical to the combination of the evolution between $\sqrt{s}$ and κ, and the evolution between κ and Q_0. For each value of the scale κ we will insert either one or two emissions, to perform a calculation of eqs. (3.14), (3.15). These are identified by the three contributions defined below. According to eq. (4.16) this scale is sampled uniformly and ensures that each insertion can occur at any possible scale along the evolution tree.

Algorithm 4.1: Insertion of $Z_{12}^{(0)}[Q;\{u\}]$ starting from the scale κ

Generate emission k_a according to Algorithm 4.2 and split the emitting dipole;
Apply Algorithm 1 with starting scale k_{ta} and evolution time (4.15);

To carry on with the calculation of $Z_{12}^{(0)}[Q;\{u\}]$ starting from Algorithm 4, we simply generate an emission k_a according to eq. (3.14) and then continue with the evolution

JHEP03(2022)135

Algorithm 4.2: Generation of emission k_a starting from the scale κ

Select an emitting dipole $\{p_{\ell_1} p_{\ell_2}\}$ for k_a as in Algorithm 1;
Generate k_{ta} as in Algorithm 1, starting from the scale κ;

from the scale of the emission all the way down to Q_0. This procedure is described in Algorithm 4.1.

Let us now move to eq. (3.15). We calculate separately the contributions proportional to $\tilde{w}_{12}^{(0)}$ and the strongly-ordered squared amplitude in eq. (3.15), starting with the former. Its calculation is addressed by Algorithm 4.3, that we now outline. We start with the truncated evolution introduced above, and starting from the truncation scale κ we generate two insertions of momenta k_a and k_b. We start by considering the two ratios of Sudakov factors $\Delta_{12}(Q)/\Delta_{12}(k_{t(ab)})$ and $\Delta_{12}(Q)/\Delta_{12}(k_{ta})$ in the second and third term in the r.h.s. of eq. (3.15), respectively. As shown in ref. [16], these two terms only contribute at NLL in the *unordered* kinematic region where $k_{ta} \sim k'_{tb} \sim k_{tb}$, while they cancel in strongly ordered regimes. We can therefore introduce an extra ratio of Sudakov factors between the scales k_{ta} and k_{tb} in the second and third terms in the r.h.s. of eq. (3.15), as it only amounts to introducing subleading logarithmic corrections since[4]

$$\mathcal{O}\left(\alpha_s \ln \frac{k_{ta}}{k_{t(ab)}}\right) \sim \mathcal{O}\left(\alpha_s \ln \frac{k_{ta}}{k_{tb}}\right) \sim \mathcal{O}\left(\alpha_s\right) . \tag{4.17}$$

Concretely, for the contributions in which k_b is emitted off dipole $\{1a\}$ we can make the replacements

$$\bar{\alpha}^2(k_{t(ab)}) \frac{\Delta_{12}(Q)}{\Delta_{12}(k_{t(ab)})} \to \bar{\alpha}(k_{ta})\bar{\alpha}(k_{tb}) \frac{\Delta_{12}(Q)}{\Delta_{12}(k_{ta})} \frac{\Delta_{1a}(k_{ta}\, k_{tb}/k'_{tb})}{\Delta_{1a}(k_{tb})} , \tag{4.18}$$

$$\bar{\alpha}^2(k_{ta}) \frac{\Delta_{12}(Q)}{\Delta_{12}(k_{ta})} \to \bar{\alpha}(k_{ta})\bar{\alpha}(k_{tb}) \frac{\Delta_{12}(Q)}{\Delta_{12}(k_{ta})} \frac{\Delta_{1a}(k_{ta})}{\Delta_{1a}(k_{tb})} , \tag{4.19}$$

in the second and third term in the r.h.s. of eq. (3.15), respectively. The complementary colour flow (i.e. k_b is emitted off dipole $\{a2\}$) is treated analogously. These approximations are unnecessary from a purely theoretical point of view (they introduce at most NNLL corrections). However, the extra ratio of Sudakov factors has the advantage of suppressing regions of phase space close to the collinear singularity, therefore guaranteeing a much improved numerical stability in the calculation. Following exactly the same reasoning, we can also replace $k_{t(ab)}$ with k_{ta} in the scale of *all* the $Z^{(0)}$ generating functionals in the second term in the r.h.s. of eq. (3.15). This also preserves the collinear safety of the latter.

In eq. (4.18), the argument of the second Sudakov is such that we can generate

$$k_{tb} \leq k_{ta} \frac{k_{tb}}{k'_{tb}} = k_{ta}\, f(p_{\ell_1}, p_{\ell_2}, \hat{k}_b) , \tag{4.20}$$

where we used

$$k'_{tb} = \frac{k_{tb}}{f(p_{\ell_1}, p_{\ell_2}, \hat{k}_b)} . \tag{4.21}$$

[4]Section 4 of ref. [16] contains a more detailed discussion about this point.

JHEP03(2022)135

Algorithm 4.3: Insertion of $Z_{12}^{(1)}[Q;\{u\}]$ starting from the scale κ

Generate emissions k_a and k_b according to Algorithms 4.2 and 4.4, respectively;
Create an *event*:
while true **do**
  if $\Theta_{\text{in}}(k_a) = 1$ *and* $\Theta_{\text{in}}(k_b) = 1$ **then**
    Reconstruct $k_{(ab)}$ with eq. (2.26);
    Fill the histogram with $V(k_{(ab)})$ iff $\Theta_{\text{in}}(k_{(ab)}) = 1$ and break;
  else if $\Theta_{\text{in}}(k_a) = 1$ *or* $\Theta_{\text{in}}(k_b) = 1$ **then**
    Fill the histogram with either $V(k_a)$ or $V(k_b)$ and break;
  end
  Split the emitting dipole into three adjacent dipoles according to k_a and k_b;
  Apply Algorithm 1 with starting scale k_{ta} and evolution time (4.15);
  break;
end
Create a *counter-event*:
Set $w \mathrel{*}= -1$;
while true **do**
  Reconstruct $k_{(ab)}$ with eq. (2.26);
  Replace k_a with $k_{(ab)}$;
  if $\Theta_{\text{in}}(k_{(ab)}) = 1$ **then**
    Fill the histogram with $V(k_{(ab)})$ and break;
  end
  Split the emitting dipole into two adjacent dipoles according to $k_{(ab)}$;
  Apply Algorithm 1 with starting scale k_{ta} and evolution time (4.15);
  break;
end

The function $f(p_{\ell_1}, p_{\ell_2}, \hat{k}_b)$, defined in eq. (4.22), exclusively depends on the directions of the momenta p_{ℓ_1}, p_{ℓ_2}, k_b and not on their energies. Eq. (4.20) arises from requiring $k'_{tb} < k_{ta}$. The first (k_a) and second (k_b) insertions are then generated according to Algorithms 4.2 and 4.4, respectively.

We then calculate the difference of terms proportional to $\tilde{w}_{12}^{(0)}$ in eq. (3.15). An important remark concerns the construction of the $k_{(ab)}$ momentum appearing in the counter-term in eq. (3.15). This momentum is introduced in eq. (2.26) where it is defined in the rest frame of the dipole that radiates the pair k_a, k_b (with dipole axis along the z direction), and needs to be Lorentz transformed back into the event frame. All Lorentz transformations are performed as described in section 4.1, using momenta with unit energy. A last comment about the procedure to fill the histograms in Algorithm 4.3 is in order. In particular, in order to eliminate NNLL contributions, when both insertions k_a and k_b are in the interjet rapidity gap in the *event* we consider the observable calculated on the massless parent defined in eq. (2.26). This procedure exactly reproduces what is done in the *counter-event*,

JHEP03(2022)135

and therefore ensures that for the NNLL configurations in which both insertions are in the gap the two contributions cancel by construction.

Finally, the remaining contribution to the evolution (3.15) of $Z_{12}^{(1)}[Q;\{u\}]$, proportional to the strongly ordered double-soft squared amplitude ($w_{12}^{(0)}w_{a2}^{(0)}$ and $w_{12}^{(0)}w_{1a}^{(0)}$), is also obtained with Algorithm 4.3. Here one must replace all instances of $k_{(ab)}$ with k_a, and generate k_b with the simpler constraint $k_{tb} < k_{ta}$, which is obtained by setting the angular function $f(p_{\ell_1}, p_{\ell_2}, \hat{k}_b) \to 1$ in eq. (4.22). Moreover, we set the weight according to the strongly-ordered limit of eq. (4.23) (cf. eq. (3.15)), that simply amounts to removing the reweighing step (4.23) altogether. This guarantees that the iteration of the LL evolution kernel in (3.14) is correctly subtracted. The final result for $\mathcal{H}_2 \otimes S_2(v)$ is then obtained as the sum of the result of the above three contributions.

Algorithm 4.4: Generation of emission k_b starting from the scale k_{ta}

Pick the dipole that emits k_b among $\{p_{\ell_1}k_a\}$ and $\{k_a p_{\ell_2}\}$ with probability 1/2;

Update weight $w \mathrel{*}= 2$;

Generate k_{tb} w.r.t. the emitting dipole as in Algorithm 1 starting from the scale

$$k_{ta}\, f(p_{\ell_1}, p_{\ell_2}, \hat{k}_b)\,, \quad f(p_{\ell_1}, p_{\ell_2}, \hat{k}_b) \coloneqq \sqrt{\frac{(p_{\ell_1}\cdot p_{\ell_2})}{2(p_{\ell_1}\cdot \hat{k}_b)(\hat{k}_b \cdot p_{\ell_2})}}\,, \tag{4.22}$$

where $\hat{k}_b$ denotes k_b with its k_t w.r.t. the emitting dipole set to one;

Update the weight

$$w \mathrel{*}= \frac{\tilde{w}_{12}^{(0)}(k_b, k_a)}{w_{12}^{(0)}(k_a) w_{1a}^{(0)}(k_b)}\,; \quad w \mathrel{*}= \frac{\tilde{w}_{12}^{(0)}(k_a, k_b)}{w_{12}^{(0)}(k_a) w_{a2}^{(0)}(k_b)}\,, \tag{4.23}$$

for the two dipoles, respectively;

5 Numerical results for the E_t distribution in the interjet gap at NLL

In this section we apply the technique described in section 4 to the calculation of the transverse energy distribution in the rapidity gap between the two cone jets in e^+e^-. In the following we set $\sqrt{s} = M_Z$ and adopt the value $\alpha_s(M_Z) = 0.118$ for the strong coupling constant. To obtain a physical prediction for this observable, we introduce the standard perturbative scales used in resummed calculations whose variation quantifies the size of subleading logarithmic corrections. These are discussed in appendix B. We vary the renormalisation scale μ_R by a factor of two around its central value $\mu_R = \sqrt{s}$, and for central μ_R, we also vary the resummation scale μ_Q by a factor of two around its central value $\mu_Q = \sqrt{s}/2$. The final perturbative uncertainty shown in the results that follow is obtained as the envelope of the above five predictions. The calculation performed in this section is strictly speaking valid only in the limit of soft radiation, and therefore should be consistently matched to a fixed order calculation in the bulk of the phase space where the

JHEP03(2022)135

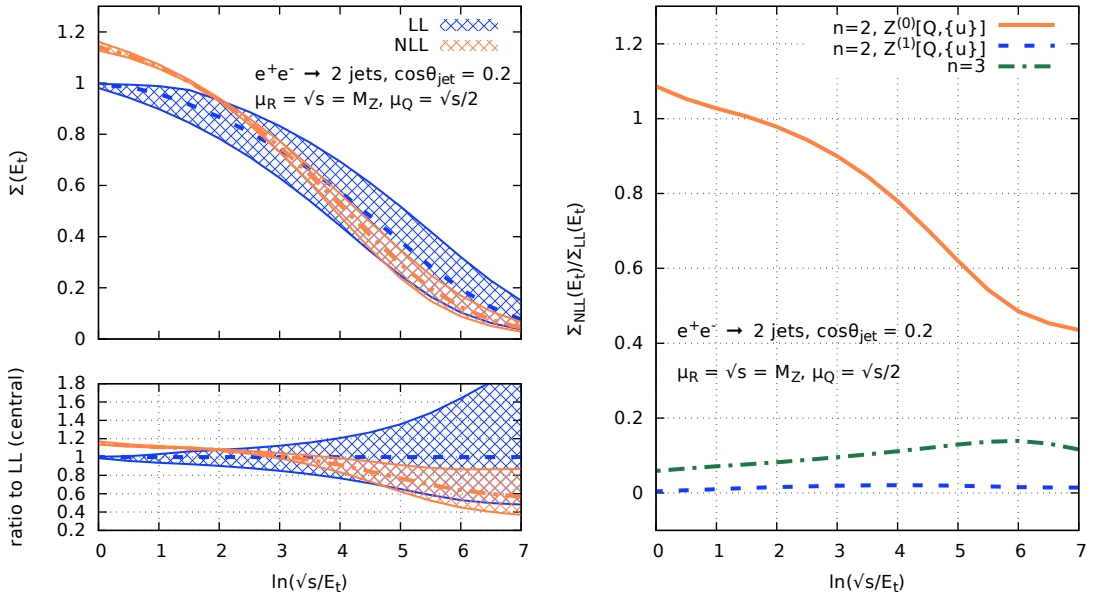

Figure 3. Left: cumulative distribution $\Sigma(E_t)$ for the transverse energy in the interjet rapidity gap at LL and NLL for $c = 0.2$. Right: breakdown of the contributions to the NLL correction, relative to the LL prediction.

emitted radiation is hard. A matching of this type is standard in resummed calculation and must be performed in future phenomenological applications.

As a check of our calculation, we have also computed the LL $\Sigma(v)$ cumulative distribution as a function of the evolution variable t defined in eq. (4.4), and reproduced the results of ref. [2]. Notice that the LL evolution time (4.4) is defined in terms of the *dipole* transverse momentum of the gluon that is radiated inside the interjet rapidity gap. This transverse momentum is related to the physical observable E_t via an $\mathcal{O}(1)$ angular function that depends on the orientation of the emitting dipole w.r.t. the thrust axis, that varies on an event-by-event basis. Therefore the relation between t and E_t is not bijective. In ref. [16] we have also compared the $\mathcal{O}(\alpha_s^2)$ expansion of our calculation to fixed-order predictions in full QCD, finding excellent agreement in the limit of $E_t \to 0$. In the same article, we have also verified that our fixed-order expansion for the energy distribution E reproduces the calculation of ref. [13]. As a further check, we have carried out two independent implementations of the algorithms given in section 4 and found complete agreement. A public version of the code can be found in ref. [65].

In the left plots of figures 3, 4, 5, we report the cumulative distribution (2.2) at LL and NLL for three different values for the width of the interjet rapidity gap ($\cos\theta_{\text{jet}} = c = \{0.2, 0.5, 0.9\}$), which correspond to different opening angles of the two hard jets (cf. eq. (2.1)). We observe that the definition of the infrared scale Q_0 in eq. (4.5) (introduced in our prescription to deal with the Landau singularity in eq. (2.31)) acts as a cutoff on the transverse momentum of the emissions w.r.t. the emitting dipole. Therefore, the region of

JHEP03(2022)135

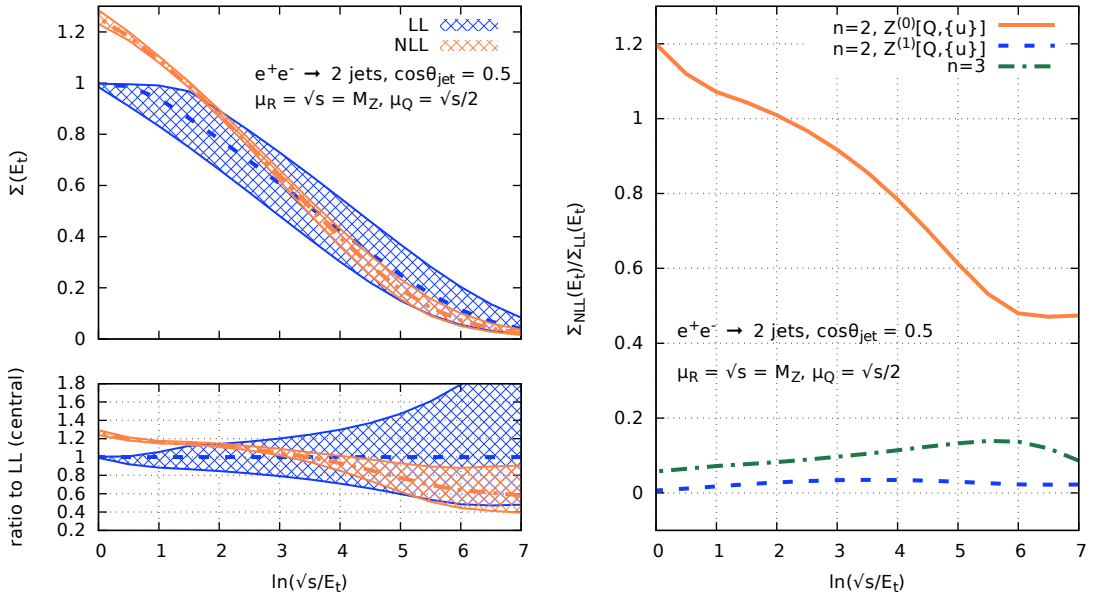

Figure 4. Left: cumulative distribution $\Sigma(E_t)$ for the transverse energy in the interjet rapidity gap at LL and NLL for $c = 0.5$. Right: breakdown of the contributions to the NLL correction, relative to the LL prediction.

the plots in which the observable $E_t \sim Q_0$ (and below) is susceptible to non-perturbative effects. We therefore truncate the plots at this scale (i.e. $\ln(\sqrt{s}/E_t) = 1/(2\alpha_s\beta_0) \simeq 7$) cutting out the non-perturbative region. We start by considering the region of the plots that corresponds to a large transverse energy inside the interjet rapidity gap. The predictivity here is restored upon a matching to a fixed-order calculation, which however is not performed in figures 3, 4, 5. We therefore do not comment further on this region and we rather focus on the small E_t regime, where (non-global) resummation effects are dominant. We notice, however, that the normalisation of the curves at large E_t changes with the size of the cone jets. This can understood by observing the c-dependence of the hard factors $\mathcal{H}_2$ and $\mathcal{H}_3$ calculated in section 4. The residual scale dependence at large E_t present at NLL is due to the μ_R dependence of the hard factors, which is absent by construction at LL. At small E_t, we observe that NLL corrections are large and negative, and reach 40% in size when the resummed logarithms are large, consistently across different values of the jet cone size. We stress that the results presented here adopt the physical E_t definition for the LL calculation rather than its strict leading-logarithmic limit in which E_t is simply the dipole tranverse momentum of the emission in the interjet gap. In the latter case, the size of the genuine NLL corrections would be even larger as these would also compensate for the kinematical difference between the dipole k_t and the actual definition of E_t. We also observe a substantial reduction of the perturbative uncertainty, up to a factor of two, in the NLL calculation compared to the LL prediction, whose uncertainty band however accounts for the large NLL corrections. We have also checked the stability of our predictions with

JHEP03(2022)135

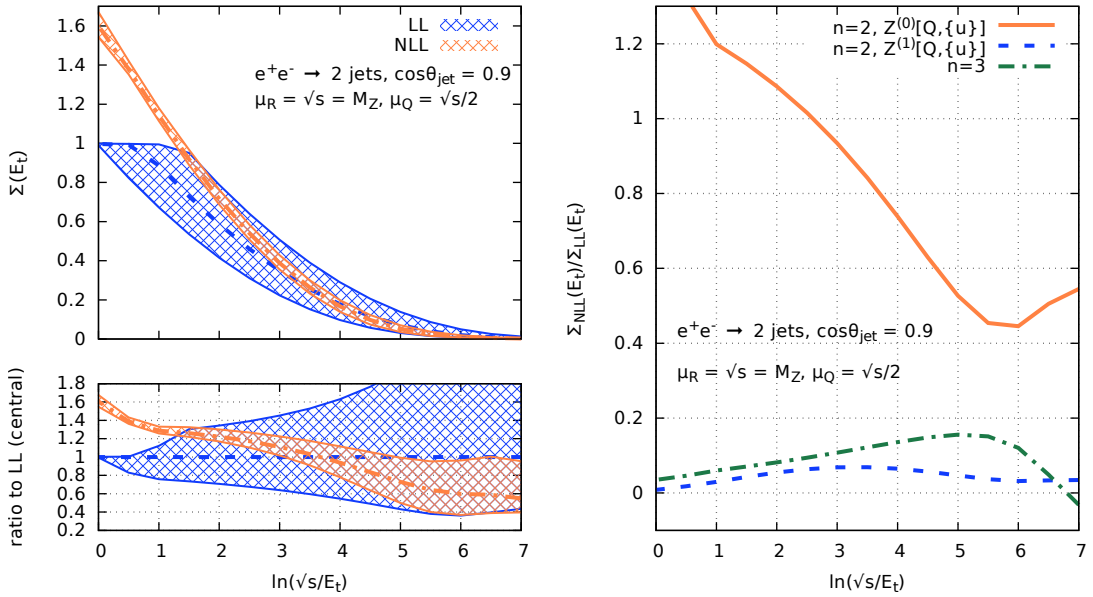

Figure 5. Left: cumulative distribution $\Sigma(E_t)$ for the transverse energy in the interjet rapidity gap at LL and NLL for $c = 0.9$. Right: breakdown of the contributions to the NLL correction, relative to the LL prediction.

respect to variations of the non-perturbative cutoff Q_0, defined in eq. (4.5). Specifically, in that equation we replace Q_0 with Q_0/X, and we vary X in the range $1 \leq X \leq 2$. We observe a moderate dependence for small values of E_t approaching the Landau pole. This dependence is however well within the scale uncertainty band. Finally, as a measure of the numerical complexity of the calculations shown here, we computed the average gluon multiplicity in the events as a function of $\ln(\sqrt{s}/E_t)$. We find that the multiplicity strongly depends on $\ln(\sqrt{s}/E_t)$, it reaches a maximum of about 20-25 for the narrow slice, and decreases significantly for broader slices. This behaviour is expected since the evolution stops as soon as any radiation populates the interjet rapidity slice.

It is informative to study the size of the various contributions to the NLL corrections to the cumulative distribution. In the right plots of figures 3, 4, 5, we then show the breakdown of the NLL correction into three different pieces. These are the $\mathcal{H}_n \otimes S_n(v)$ terms in eq. (2.3), with $n = 2$ and $n = 3$. Moreover, for $n = 2$, we plot separately the contribution from the functional $Z_{12}^{(0)}$, defined in eq. (3.14), and $Z_{12}^{(1)}$, defined in eq. (3.15). We observe that for small interjet gaps, i.e. fat cone jets, the NLL result is completely dominated by the $Z_{12}^{(0)}$ correction, with an additional sizeable correction from the $\mathcal{H}_3 \otimes S_3(v)$ term. For larger c values (corresponding to narrower jets), however, the contribution of the $Z_{12}^{(1)}$ correction slightly grows and becomes comparable to that of the $\mathcal{H}_3 \otimes S_3(v)$ term at small values of E_t. The moderate contribution of the $Z_{12}^{(1)}$ correction compared to $Z_{12}^{(0)}$ justifies entirely the perturbative approach adopted in eq. (3.13) for the generating functional Z_{12} which led to the evolution equations (3.14) and (3.15).

JHEP03(2022)135

6 Conclusions

In this article we have presented the first NLL resummation for non-global radiative corrections to a collider observable in the large-N_c limit. We considered a set of evolution equations that we derived in a recent article, describing the dynamics of soft gluons emitted at large angles with respect to the hard scattering process. To solve these equations numerically, we have reformulated the resummation in terms of generating functionals, which can be used for the calculation of the emission probability associated with any given final state containing n soft gluons. This formulation is suitable for a numerical implementation by means of Monte Carlo methods. Using this technology, we have presented an algorithm for the solution of the evolution equations, hence achieving the resummation of NLL non-global corrections. We applied this formalism to the calculation of the NLL distribution of the transverse energy E_t of the radiation within the gap between two hard cone jets produced in e^+e^- collisions. We found that the NLL corrections are rather sizeable and their inclusion leads to a substantial reduction of the perturbative scale uncertainties in the theoretical calculation. They do therefore play an important role in the accurate prediction of this class of observables at particle colliders.

We point out that the algorithms presented in this article are not tailored to the specific observable considered here, and are directly applicable to hadron-collider observables in the large-N_c approximation. This is because the only process dependence occurs in the hard factors $\mathcal{H}_n$ of eq. (2.3) (which in turn can be calculated algorithmically for a given process), while the evolution of the soft factors S_n with the energy scale is entirely process independent as expected from the factorisation of squared amplitudes in the soft limit. Therefore, the formalism presented here can be applied to all observables that are solely sensitive to soft radiation emitted with large angles from the hard scattering, which are characterised by a single logarithmic perturbative expansion, i.e. the dominant logarithmic tower in the cumulative distribution is of the form $\alpha_s^n L^n$. The application to observables sensitive to collinear radiation, on the other hand, requires extra care since the formulation presented here must be supplemented with the correct resummation of the corresponding collinear logarithms (obtained for instance with standard techniques for global observables), and the double counting between the two regions (i.e. the soft and collinear limit) must be consistently subtracted in the evolution equations for the generating functionals. This subtraction is simple for most observables, and it simply amounts to dividing the cumulative distribution (2.3) by the contribution from *primary* radiation. This is obtained by running the algorithms given in section 4 while forbidding the dipoles to split, so that all emissions are radiated off the primary $q\bar{q}$ dipole. However, we notice that there might be cases in which the subtraction becomes conceptually more delicate, such as in the case of observables affected by abelian *clustering* logarithms [66]. The technical details of these subtraction procedures, as well as the application to hadronic observables is left for future work.

The computer code GNOLE [65] used to perform the calculations presented in this article can be downloaded from the repository:

https://github.com/non-global/gnole.

JHEP03(2022)135

Acknowledgments

We are grateful to Gavin Salam for several useful discussions through the course of this work, and to Mrinal Dasgupta, Keith Hamilton, Gavin Salam, and Gregory Soyez for numerous exchanges about conceptual aspects of non-global resummation and its Monte Carlo implementation. We would also like to thank Mrinal Dasgupta and Gavin Salam for sharing with us the computer code developed in ref. [2], that we used as a benchmark and for comparisons in our numerical tests, as well as for their constructive comments on the article. This work was supported by the Science Technology and Facilities Council (STFC) under grants number ST/T00102X/1 (AB) and ST/T000864/1 (FD), as well as by a Royal Society Research Professorship (RP\R1\180112) and University Research Fellowship (URF\R1\211294) (FD).

A Symmetries of the squared amplitude and choice of ordering

In this appendix we comment on the choice of the dipole k_t as ordering variable for the evolution equation. Let us start by considering the emission of two soft gluons in the strongly ordered limit, and we focus on the double-real integral

$$\frac{1}{2!}\int[dk_a]\int[dk_b]\left[w_{12}^{(0)}(k_a)w_{1a}^{(0)}(k_b)+w_{12}^{(0)}(k_a)w_{a2}^{(0)}(k_b)\right]u(k_a)u(k_b)\,. \tag{A.1}$$

We now introduce a partition of unity using the *dipole* transverse momentum

$$1=\Theta(k_{ta}-k_{tb})+\Theta(k_{tb}-k_{ta})\,. \tag{A.2}$$

We stress that the dipole k_{tb} is defined differently in the two colour flow configurations of eq. (A.1), following eq. (2.28), which highlights the non-trivial nature of the partition (A.2). In order to write a Monte Carlo algorithm that iterates correctly the squared amplitude, the two regions in eq. (A.2) must be identical (or at least in the kinematic limits relevant to a given logarithmic accuracy), so that the combinatorial factor 1/2! in eq. (A.1) can be effectively replaced with a kinematic ordering. To show that dipole k_t ordering is a suitable choice, we observe that the squared amplitude in the strongly-ordered limit satisfies the symmetry (e.g. in the case of two emissions)

$$\mathbb{T}\coloneqq\{\hat{n}_a\leftrightarrow\hat{n}_b;k_{tb}\leftrightarrow k_{ta}\}\,, \tag{A.3}$$

where the transverse momenta are always meant w.r.t. the emitting dipole and the directions $\hat{n}_{a,b}$ are taken in the $\{12\}$ dipole frame. This symmetry is highly non trivial, and it is now interesting to understand how the integrand in eq. (A.1) behaves under its action. We consider separately the two colour flows

$$1):\quad\{1,a,b,2\}\,,\qquad 2):\quad\{1,b,a,2\}\,, \tag{A.4}$$

and define the transformation $\mathbb{T}^{(i)}$ $(i=1,2)$ such that for each colour flow we can obtain the transformed momenta $\tilde{k}_{a,b}$ as

$$\begin{bmatrix}\tilde{k}_a\\ \tilde{k}_b\end{bmatrix}=\mathbb{T}^{(i)}\begin{bmatrix}k_a\\ k_b\end{bmatrix}\,. \tag{A.5}$$

JHEP03(2022)135

Imposing the constraints of eq. (A.3) leads to

$$\mathbb{T}^{(1)} = \begin{bmatrix} 0 & \left(\frac{(p_1\cdot k_b)(k_a\cdot p_2)}{(p_1\cdot p_2)(k_a\cdot k_b)}\right)^{-1/2} \\ \left(\frac{(p_1\cdot k_a)(k_b\cdot p_2)}{(p_1\cdot p_2)(k_a\cdot k_b)}\right)^{1/2} & 0 \end{bmatrix}, \tag{A.6}$$

$$\mathbb{T}^{(2)} = \begin{bmatrix} 0 & \left(\frac{(p_1\cdot k_a)(k_b\cdot p_2)}{(p_1\cdot p_2)(k_a\cdot k_b)}\right)^{-1/2} \\ \left(\frac{(p_1\cdot k_b)(k_a\cdot p_2)}{(p_1\cdot p_2)(k_a\cdot k_b)}\right)^{1/2} & 0 \end{bmatrix}. \tag{A.7}$$

In the above matrices $\mathbb{T}^{(i)}$ each entry is to be understood to be proportional to the identity operator that acts on the four momenta as in eq. (A.5). Let us also work out the action of the above transformation on the phase space measure. We find

$$\mathbb{T}^{(1)}\,[[dk_a][dk_b]] = \frac{(p_1\cdot k_a)(k_b\cdot p_2)}{(p_1\cdot k_b)(p_a\cdot p_2)}\,[dk_a][dk_b]\,,\quad \mathbb{T}^{(2)}\,[[dk_a][dk_b]] = \frac{(p_1\cdot k_b)(k_a\cdot p_2)}{(p_1\cdot k_a)(k_b\cdot p_2)}\,[dk_a][dk_b]\,. \tag{A.8}$$

The strongly ordered squared amplitude is invariant under the above trasformations *for each separate dipole*, a consequence of the conformal symmetry of the integrand in the presence of strongly ordered kinematics. However, due to the non-trivial effect of $\mathbb{T}$ on the phase space measure, the LL integrand itself is *not* invariant. By applying the transformation to the integrand we find (e.g. for dipole 1)

$$\mathbb{T}^{(1)}\left[[dk_a][dk_b]w_{12}^{(0)}(k_a)w_{a2}^{(0)}(k_b)\right] = [dk_a][dk_b]w_{12}^{(0)}(k_a)w_{1a}^{(0)}(k_b)\,, \tag{A.9}$$

that is the transformation simply maps the integrand into the one corresponding to the complementary colour configuration. This implies that the full LL integrand, given by the sum of the different dipoles is indeed invariant under $\mathbb{T}$, and that therefore the transverse momentum taken w.r.t. the emitting dipole can be adopted as an evolution variable as done in eq. (2.12).

At NLL we need to consider unordered configurations in which the two emissions k_a and k_b are described by the full double-soft squared amplitude in large-N_c $\tilde{w}_{12}^{(0)}(k_a,k_b) + \tilde{w}_{12}^{(0)}(k_b,k_a)$ (see eq. (2.24)). This squared amplitude is not invariant under the $\mathbb{T}$ transformations, indicating that dipole k_t ordering cannot be used for the calculation of the double-real correction (2.22). Instead, one can order the emissions k_a and k_b using their transverse momenta w.r.t. the $\{12\}$ dipole k_{ta}, k'_{tb}, under which the squared amplitude is fully symmetric. This explains the factor $\Theta(k_{ta}-k'_{tb})$ in eq. (2.22). An alternative solution would be to formulate the whole evolution ordered in *energy*, which would allow one to use the same ordering in the strongly ordered limit as well as in unordered kinematic configurations.

B Dependence on the perturbative scales μ_R and μ_Q

In this appendix we introduce the renormalisation μ_R and resummation μ_Q scales. In general, there are two sources of μ_R dependence, which appears both in the hard factors $\mathcal{H}_2$ and $\mathcal{H}_3$ as well as in the soft factors S_2 and S_3 (or equivalently in the generating functionals $Z_{12}[Q;\{u\}]$, $Z_{13}[Q;\{u\}]$ and $Z_{23}[Q;\{u\}]$ in eq. (3.3)).

JHEP03(2022)135

For the physical process under consideration, the μ_R dependence in the hard factors is entirely encoded in the $\overline{\text{MS}}$ coupling

$$\alpha_s \to \alpha_s(\mu_R)\,. \tag{B.1}$$

Extra dependence on μ_R in $\mathcal{H}_2$ and $\mathcal{H}_3$ arises for processes which are mediated by QCD interactions at the Born level, such as jet production at hadron colliders. The second source of μ_R dependence is given by the generating functionals. This is introduced by expressing $\bar{\alpha}(k_t)$ in terms of $\bar{\alpha}\left(\frac{\mu_R}{\sqrt{s}}k_t\right)$ in eq. (3.6), and then expanding out the result in $\bar{\alpha}\,(\mu_R)$ at *fixed* $\bar{\alpha}\,(\mu_R)\ln\frac{\sqrt{s}}{k_t} \sim 1$. The running of the coupling must match the logarithmic order of the calculation, and therefore we use one-loop running at LL and two-loop running at NLL.

The resummation scale μ_Q is introduced to estimate the size of subleading logarithmic corrections. Its dependence is entirely encoded in the soft factors, and thus in the generating functional. The whole μ_R and μ_Q scale dependence can be easily encoded in the evolution algorithms presented in section 3. Specifically, it amounts to replacing the evolution times (4.4) (4.15) with

$$t \to\ \tilde{t} := -\frac{N_c}{2\pi\beta_0}\ln\left(1-2\tilde{\lambda}\right)\,, \qquad \tilde{\lambda} = \beta_0\alpha_s(\mu_R)\ln\frac{\mu_Q}{k_t}\,, \tag{B.2}$$

$$\begin{aligned} t \to\ \tilde{t} := &-\frac{N_c}{2\pi\beta_0}\ln\left(1-2\tilde{\lambda}\right) + \bar{\alpha}(\mu_R)\frac{\tilde{\lambda}}{1-2\tilde{\lambda}}\ln\frac{\mu_R^2}{\mu_Q^2} + \bar{\alpha}(\mu_R)\ln\frac{\sqrt{s}}{\mu_Q} \\ &+ \bar{\alpha}(\mu_R)\left[\frac{\tilde{\lambda}}{1-2\tilde{\lambda}}\left(\frac{K^{(1)}}{2\pi\beta_0}-\frac{\beta_1}{\beta_0^2}\right) - \frac{\ln(1-2\tilde{\lambda})}{1-2\tilde{\lambda}}\frac{\beta_1}{2\beta_0^2}\right] + \mathcal{O}(\text{NNLL})\,, \end{aligned} \tag{B.3}$$

at LL and NLL, respectively. The definition of the infrared scale Q_0 given in eq. (4.5) is also consistently modified as follows

$$2\,\beta_0\alpha_s(\mu_R)\ln\frac{\mu_Q}{Q_0} = 1\,. \tag{B.4}$$

References

[1] M. Dasgupta and G.P. Salam, *Resummation of nonglobal QCD observables*, *Phys. Lett. B* **512** (2001) 323 [hep-ph/0104277] [INSPIRE].

[2] M. Dasgupta and G.P. Salam, *Accounting for coherence in interjet E(t) flow: A Case study*, *JHEP* **03** (2002) 017 [hep-ph/0203009] [INSPIRE].

[3] A. Banfi, G. Marchesini and G. Smye, *Away from jet energy flow*, *JHEP* **08** (2002) 006 [hep-ph/0206076] [INSPIRE].

[4] Y. Hatta and T. Ueda, *Resummation of non-global logarithms at finite N_c*, *Nucl. Phys. B* **874** (2013) 808 [arXiv:1304.6930] [INSPIRE].

JHEP03(2022)135

[5] Y. Hagiwara, Y. Hatta and T. Ueda, *Hemisphere jet mass distribution at finite N_c*, *Phys. Lett. B* **756** (2016) 254 [arXiv:1507.07641] [INSPIRE].

[6] Z. Nagy and D.E. Soper, *Effect of color on rapidity gap survival*, *Phys. Rev. D* **100** (2019) 074012 [arXiv:1905.07176] [INSPIRE].

[7] Y. Hatta and T. Ueda, *Non-global logarithms in hadron collisions at $N_c = 3$*, *Nucl. Phys. B* **962** (2021) 115273 [arXiv:2011.04154].

[8] M. De Angelis, J.R. Forshaw and S. Plätzer, *Resummation and Simulation of Soft Gluon Effects beyond Leading Color*, *Phys. Rev. Lett.* **126** (2021) 112001 [arXiv:2007.09648] [INSPIRE].

[9] J.R. Forshaw, A. Kyrieleis and M.H. Seymour, *Super-leading logarithms in non-global observables in QCD*, *JHEP* **08** (2006) 059 [hep-ph/0604094] [INSPIRE].

[10] J.R. Forshaw, A. Kyrieleis and M.H. Seymour, *Super-leading logarithms in non-global observables in QCD: Colour basis independent calculation*, *JHEP* **09** (2008) 128 [arXiv:0808.1269] [INSPIRE].

[11] T. Becher, M. Neubert and D.Y. Shao, *Resummation of Super-Leading Logarithms*, *Phys. Rev. Lett.* **127** (2021) 212002 [arXiv:2107.01212] [INSPIRE].

[12] T. Becher, M. Neubert, L. Rothen and D.Y. Shao, *Effective Field Theory for Jet Processes*, *Phys. Rev. Lett.* **116** (2016) 192001 [arXiv:1508.06645] [INSPIRE].

[13] T. Becher, M. Neubert, L. Rothen and D.Y. Shao, *Factorization and Resummation for Jet Processes*, *JHEP* **11** (2016) 019 [*Erratum ibid.* **05** (2017) 154] [arXiv:1605.02737] [INSPIRE].

[14] S. Caron-Huot, *Resummation of non-global logarithms and the BFKL equation*, *JHEP* **03** (2018) 036 [arXiv:1501.03754] [INSPIRE].

[15] A.J. Larkoski, I. Moult and D. Neill, *Non-Global Logarithms, Factorization, and the Soft Substructure of Jets*, *JHEP* **09** (2015) 143 [arXiv:1501.04596] [INSPIRE].

[16] A. Banfi, F.A. Dreyer and P.F. Monni, *Next-to-leading non-global logarithms in QCD*, *JHEP* **10** (2021) 006 [arXiv:2104.06416] [INSPIRE].

[17] J. Forshaw, J. Keates and S. Marzani, *Jet vetoing at the LHC*, *JHEP* **07** (2009) 023 [arXiv:0905.1350] [INSPIRE].

[18] M. Rubin, *Non-Global Logarithms in Filtered Jet Algorithms*, *JHEP* **05** (2010) 005 [arXiv:1002.4557] [INSPIRE].

[19] A. Banfi, M. Dasgupta, K. Khelifa-Kerfa and S. Marzani, *Non-global logarithms and jet algorithms in high-pT jet shapes*, *JHEP* **08** (2010) 064 [arXiv:1004.3483] [INSPIRE].

[20] R.M. Duran Delgado, J.R. Forshaw, S. Marzani and M.H. Seymour, *The dijet cross section with a jet veto*, *JHEP* **08** (2011) 157 [arXiv:1107.2084] [INSPIRE].

[21] M. Dasgupta, K. Khelifa-Kerfa, S. Marzani and M. Spannowsky, *On jet mass distributions in Z+jet and dijet processes at the LHC*, *JHEP* **10** (2012) 126 [arXiv:1207.1640] [INSPIRE].

[22] K.K. Kerfa, *QCD resummation for high-p_T jet shapes at hadron colliders*, Ph.D. Thesis, Manchester University, Manchester U.K. (2012) [arXiv:2111.10671] [INSPIRE].

[23] M.D. Schwartz and H.X. Zhu, *Nonglobal logarithms at three loops, four loops, five loops, and beyond*, *Phys. Rev. D* **90** (2014) 065004 [arXiv:1403.4949] [INSPIRE].

JHEP03(2022)135

[24] T. Becher, B.D. Pecjak and D.Y. Shao, *Factorization for the light-jet mass and hemisphere soft function*, *JHEP* **12** (2016) 018 [arXiv:1610.01608] [INSPIRE].

[25] D. Neill, *The Asymptotic Form of Non-Global Logarithms, Black Disc Saturation, and Gluonic Deserts*, *JHEP* **01** (2017) 109 [arXiv:1610.02031] [INSPIRE].

[26] S. Caron-Huot and M. Herranen, *High-energy evolution to three loops*, *JHEP* **02** (2018) 058 [arXiv:1604.07417] [INSPIRE].

[27] A.J. Larkoski, I. Moult and D. Neill, *The Analytic Structure of Non-Global Logarithms: Convergence of the Dressed Gluon Expansion*, *JHEP* **11** (2016) 089 [arXiv:1609.04011] [INSPIRE].

[28] T. Becher, R. Rahn and D.Y. Shao, *Non-global and rapidity logarithms in narrow jet broadening*, *JHEP* **10** (2017) 030 [arXiv:1708.04516] [INSPIRE].

[29] R. Ángeles Martínez, M. De Angelis, J.R. Forshaw, S. Plätzer and M.H. Seymour, *Soft gluon evolution and non-global logarithms*, *JHEP* **05** (2018) 044 [arXiv:1802.08531] [INSPIRE].

[30] M. Balsiger, T. Becher and D.Y. Shao, *Non-global logarithms in jet and isolation cone cross sections*, *JHEP* **08** (2018) 104 [arXiv:1803.07045] [INSPIRE].

[31] D. Neill, *Non-Global and Clustering Effects for Groomed Multi-Prong Jet Shapes*, *JHEP* **02** (2019) 114 [arXiv:1808.04897] [INSPIRE].

[32] M. Balsiger, T. Becher and D.Y. Shao, *NLL′ resummation of jet mass*, *JHEP* **04** (2019) 020 [arXiv:1901.09038] [INSPIRE].

[33] M. Balsiger, T. Becher and A. Ferroglia, *Resummation of non-global logarithms in cross sections with massive particles*, *JHEP* **09** (2020) 029 [arXiv:2006.00014] [INSPIRE].

[34] N. Ziani, K. Khelifa-Kerfa and Y. Delenda, *Jet mass distribution in Higgs/vector boson + jet events at hadron colliders with k_t clustering*, *Eur. Phys. J. C* **81** (2021) 570 [arXiv:2104.11060] [INSPIRE].

[35] H. Weigert, *Nonglobal jet evolution at finite N(c)*, *Nucl. Phys. B* **685** (2004) 321 [hep-ph/0312050] [INSPIRE].

[36] Y. Hatta, *Relating e^+e^- annihilation to high energy scattering at weak and strong coupling*, *JHEP* **11** (2008) 057 [arXiv:0810.0889] [INSPIRE].

[37] M. Dasgupta, F.A. Dreyer, K. Hamilton, P.F. Monni and G.P. Salam, *Logarithmic accuracy of parton showers: a fixed-order study*, *JHEP* **09** (2018) 033 [*Erratum ibid.* **03** (2020) 083] [arXiv:1805.09327] [INSPIRE].

[38] G. Bewick, S. Ferrario Ravasio, P. Richardson and M.H. Seymour, *Logarithmic accuracy of angular-ordered parton showers*, *JHEP* **04** (2020) 019 [arXiv:1904.11866] [INSPIRE].

[39] M. Dasgupta, F.A. Dreyer, K. Hamilton, P.F. Monni, G.P. Salam and G. Soyez, *Parton showers beyond leading logarithmic accuracy*, *Phys. Rev. Lett.* **125** (2020) 052002 [arXiv:2002.11114] [INSPIRE].

[40] J.R. Forshaw, J. Holguin and S. Plätzer, *Building a consistent parton shower*, *JHEP* **09** (2020) 014 [arXiv:2003.06400] [INSPIRE].

[41] S. Plätzer and I. Ruffa, *Towards Colour Flow Evolution at Two Loops*, *JHEP* **06** (2021) 007 [arXiv:2012.15215] [INSPIRE].

[42] K. Hamilton, R. Medves, G.P. Salam, L. Scyboz and G. Soyez, *Colour and logarithmic accuracy in final-state parton showers*, arXiv:2011.10054 [INSPIRE].

JHEP03(2022)135

[43] Z. Nagy and D.E. Soper, *Summations of large logarithms by parton showers*, *Phys. Rev. D* **104** (2021) 054049 [arXiv:2011.04773] [INSPIRE].

[44] Z. Nagy and D.E. Soper, *Summations by parton showers of large logarithms in electron-positron annihilation*, arXiv:2011.04777 [INSPIRE].

[45] A. Karlberg, G.P. Salam, L. Scyboz and R. Verheyen, *Spin correlations in final-state parton showers and jet observables*, *Eur. Phys. J. C* **81** (2021) 681 [arXiv:2103.16526] [INSPIRE].

[46] F. Dulat, S. Höche and S. Prestel, *Leading-Color Fully Differential Two-Loop Soft Corrections to QCD Dipole Showers*, *Phys. Rev. D* **98** (2018) 074013 [arXiv:1805.03757] [INSPIRE].

[47] L. Gellersen, S. Höche and S. Prestel, *Disentangling soft and collinear effects in QCD parton showers*, arXiv:2110.05964 [INSPIRE].

[48] K. Hamilton, A. Karlberg, G.P. Salam, L. Scyboz and R. Verheyen, *Soft spin correlations in final-state parton showers*, arXiv:2111.01161 [INSPIRE].

[49] K. Konishi, A. Ukawa and G. Veneziano, *Jet Calculus: A Simple Algorithm for Resolving QCD Jets*, *Nucl. Phys. B* **157** (1979) 45 [INSPIRE].

[50] A. Bassetto, M. Ciafaloni and G. Marchesini, *Jet Structure and Infrared Sensitive Quantities in Perturbative QCD*, *Phys. Rept.* **100** (1983) 201.

[51] Y.L. Dokshitzer, V.A. Khoze, A.H. Mueller and S.I. Troian, *Basics of perturbative QCD*, Editions Frontieres, Paris France (1991).

[52] J.M. Campbell and E.W.N. Glover, *Double unresolved approximations to multiparton scattering amplitudes*, *Nucl. Phys. B* **527** (1998) 264 [hep-ph/9710255] [INSPIRE].

[53] A. Gehrmann-De Ridder, T. Gehrmann and E.W.N. Glover, *Antenna subtraction at NNLO*, *JHEP* **09** (2005) 056 [hep-ph/0505111] [INSPIRE].

[54] A. Banfi, P.F. Monni, G.P. Salam and G. Zanderighi, *Higgs and Z-boson production with a jet veto*, *Phys. Rev. Lett.* **109** (2012) 202001 [arXiv:1206.4998] [INSPIRE].

[55] A. Banfi, H. McAslan, P.F. Monni and G. Zanderighi, *A general method for the resummation of event-shape distributions in e^+e^- annihilation*, *JHEP* **05** (2015) 102 [arXiv:1412.2126] [INSPIRE].

[56] A. Banfi, H. McAslan, P.F. Monni and G. Zanderighi, *The two-jet rate in e^+e^- at next-to-next-to-leading-logarithmic order*, *Phys. Rev. Lett.* **117** (2016) 172001 [arXiv:1607.03111] [INSPIRE].

[57] A. Banfi, B.K. El-Menoufi and P.F. Monni, *The Sudakov radiator for jet observables and the soft physical coupling*, *JHEP* **01** (2019) 083 [arXiv:1807.11487] [INSPIRE].

[58] P.F. Monni, L. Rottoli and P. Torrielli, *Higgs transverse momentum with a jet veto: a double-differential resummation*, *Phys. Rev. Lett.* **124** (2020) 252001 [arXiv:1909.04704] [INSPIRE].

[59] G. Gustafson and U. Pettersson, *Dipole Formulation of QCD Cascades*, *Nucl. Phys. B* **306** (1988) 746 [INSPIRE].

[60] L. Lönnblad, *ARIADNE version 4: A Program for simulation of QCD cascades implementing the color dipole model*, *Comput. Phys. Commun.* **71** (1992) 15 [INSPIRE].

[61] T. Sjöstrand and P.Z. Skands, *Transverse-momentum-ordered showers and interleaved multiple interactions*, *Eur. Phys. J. C* **39** (2005) 129 [hep-ph/0408302] [INSPIRE].

JHEP03(2022)135

[62] W.T. Giele, D.A. Kosower and P.Z. Skands, *A simple shower and matching algorithm*, *Phys. Rev. D* **78** (2008) 014026 [arXiv:0707.3652] [INSPIRE].

[63] S. Höche and S. Prestel, *The midpoint between dipole and parton showers*, *Eur. Phys. J. C* **75** (2015) 461 [arXiv:1506.05057] [INSPIRE].

[64] M. Cacciari, F.A. Dreyer, A. Karlberg, G.P. Salam and G. Zanderighi, *Fully Differential Vector-Boson-Fusion Higgs Production at Next-to-Next-to-Leading Order*, *Phys. Rev. Lett.* **115** (2015) 082002 [*Erratum ibid.* **120** (2018) 139901] [arXiv:1506.02660] [INSPIRE].

[65] A. Banfi, F. Dreyer and P. Monni, GNOLE, zenodo (2021).

[66] A. Banfi and M. Dasgupta, *Problems in resumming interjet energy flows with k_t clustering*, *Phys. Lett. B* **628** (2005) 49 [hep-ph/0508159] [INSPIRE].

JHEP03(2022)135